PORTLAND PRESS

Research Article

Peroxiredoxin 1 (Prx1) is a dual-function enzyme by possessing Cys-independent catalase-like activity

Cen-Cen Sun[1], Wei-Ren Dong[1], Tong Shao[1], Jiang-Yuan Li[1], Jing Zhao[1], Li Nie[1], Li-Xin Xiang[1], Guan Zhu[1,2] and Jian-Zhong Shao[1]

[1]College of Life Sciences, Zhejiang University, and Key Laboratory for Cell and Gene Engineering of Zhejiang Province, Hangzhou 310058, China and [2]Department of Veterinary Pathobiology, College of Veterinary Medicine & Biomedical Sciences, Texas A&M University, 4467 TAMU, College Station, Texas 77843, U.S.A.

Correspondence: Jian-Zhong Shao (shaojz@zju.edu.cn), Guan Zhu (gzhu@cvm.tamu.edu) or Li-Xin Xiang (xianglx@zju.edu.cn)

OPEN ACCESS

Peroxiredoxin (Prx) was previously known as a Cys-dependent thioredoxin. However, we unexpectedly observed that Prx1 from the green spotted puffer fish *Tetraodon nigroviridis* (TnPrx1) was able to reduce H_2O_2 in a manner independent of Cys peroxidation and reductants. This study aimed to validate a novel function for Prx1, delineate the biochemical features and explore its antioxidant role in cells. We have confirmed that Prx1 from the puffer fish and humans truly possesses a catalase (CAT)-like activity that is independent of Cys residues and reductants, but dependent on iron. We have identified that the GVL motif was essential to the CAT-like activity of Prx1, but not to the Cys-dependent thioredoxin peroxidase (POX) activity, and generated mutants lacking POX and/or CAT-like activities for individual functional validation. We discovered that the TnPrx1 POX and CAT-like activities possessed different kinetic features in the reduction of H_2O_2. The overexpression of wild-type TnPrx1 and mutants differentially regulated the intracellular levels of reactive oxygen species (ROS) and the phosphorylation of p38 in HEK-293T cells treated with H_2O_2. Prx1 is a dual-function enzyme by acting as POX and CAT with varied affinities towards ROS. This study extends our knowledge on Prx1 and provides new opportunities to further study the biological roles of this family of antioxidants.

Introduction

Peroxiredoxins (Prxs or Prdxs) are a family of ubiquitous antioxidant enzymes known to be involved in sensing and detoxifying hydrogen peroxide (H_2O_2) and other reactive oxygen species (ROS) in all kingdoms of life [1–3]. Mammalian Prxs also participate in the regulation of signal transduction by controlling the cytokine-induced peroxide levels [4–6]. Humans and other mammals possess six Prx isoforms, including four typical 2-cysteine (2-Cys Prxs) (Prx1–4), an atypical 2-Cys Prx5 and a 1-Cys Prx6 [7–9]. The thioredoxin peroxidase (POX) activity is the hallmark of Prx proteins. In the case of Prx1–4, the conserved N-terminal peroxidatic Cys residue (C_P-SH), corresponding to the Cys^{51} in the mammalian Prx1, is oxidized by H_2O_2 to cysteine sulfenic acid (C_P-SOH) and then resolved by a reaction with the C-terminal resolving Cys^{172} (C_R-SH) in the adjacent monomer to form a disulfide-bond Cys^{51} and Cys^{172} (Figure 1, Pathway II). The disulfide linkage is reduced by NADPH-dependent thioredoxin (Trx)/thioredoxin reductase (TrxR) cycles to complete the Prx catalytic cycle in cells, or by a reducing agent such as dithiothreitol (DTT) commonly used in assaying POX activity [10–12]. Alternatively, the C_P-SH and C_R-SH residues in *Homo sapiens* Prx1 (HsPrx1) can be glutathionylated in the presence of a small amount of H_2O_2, and deglutathionylated by sulfiredoxin (Srx) or glutaredoxin I (Grx I) (Figure 1, Pathway I). C_P-SH may also be hyperoxidized in the presence of excessive amount of H_2O_2 to form reversible sulfinic acid (C_P-SO$_2$H) that can be slowly recycled by Srx, or irreversible sulfonic acid (C_P-SO$_3$H), resulting in the loss of the POX activity and the formation of Prx1

1373
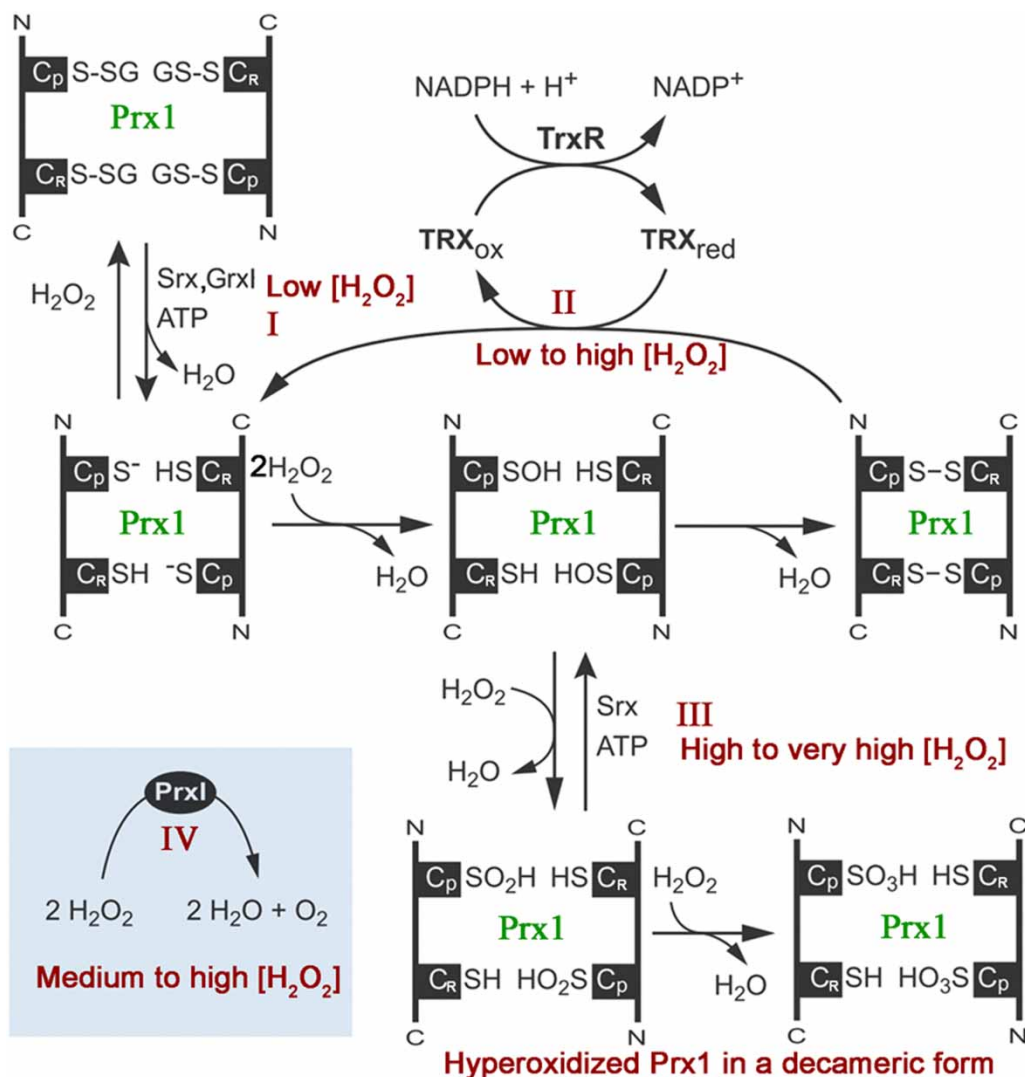
Figure 1. Illustration of pathways regulating vertebrate peroxiredoxin 1 (Prx1) to scavenge hydrogen peroxide.
Pathway I, the peroxidatic cysteine (C_P-SH) and resolving cysteine (C_R-SH) of *Homo sapiens* Prx1 (HsPrx1) can be glutathionylated in the presence of a small amount of H_2O_2, and deglutathianylated by sulfiredoxin (Srx) or glutaredoxin I (GrxI).
Pathway II, the C_P-SH of Prx1 is oxidized by H_2O_2 to cysteine-sulfenic acid (C_P-SOH), which then reacts with C_R-SH of the other subunit to produce an intermolecular disulfide, and the reducing equivalents for such typical peroxidase activity of Prx1 are ultimately derived from NADPH (reduced form of nicotinamideadenine dinucleotide phosphate) via thioredoxin reductase (TrxR) and Trx. **Pathway III**, the C_P-SH is selectively oxidized by H_2O_2 to C_P-SO$_2$H or even C_P-SO$_3$H, which can be reversed by Srx and ATP (adenosine triphosphate). **Pathway IV**, the newly discovered catalase-like activity of Prx1, which directly converts H_2O_2 to O_2.

decamers with protein chaperone function (Figure 1, Pathway III) [13–17]. Among these reactions, the rapid recycling of POX activity is responsible for the reduction of H_2O_2 and other ROS, while the other two appear to be involved in the regulation of Prx functions [18].

Although Prxs could be oxidized in multiple ways, all these POX activities were known to rely on the Cys-dependent peroxidation cycles. However, in the present study, we unexpectedly observed that the Prx1 from the green spotted puffer fish *Tetraodon nigroviridis* (TnPrx1) was able to reduce H_2O_2 in a manner that was independent of Cys peroxidation and occurred in the absence of reducing agents. This Cys-independent activity observed in wild-type (WT) and site-mutated TnPrx1 proteins differs from the classic POX activity in Prxs, but resembles the catalase (CAT)-like activity (i.e. directly reducing H_2O_2 into H_2O with the release of

O_2; or $2 H_2O_2 \rightarrow 2 H_2O + O_2$ for CAT-like activity vs. $2 H_2O_2 \rightarrow 2 H_2O$ for POX activity), making Prx1 a dual antioxidant protein. For clarity, we denoted Cys-dependent POX and Cys-independent CAT-like activities in TnPrx1 as TnPrx1-POX and TnPrx1-CAT, respectively. We have determined detailed kinetic features on the TnPrx1-CAT activity, and also identified that the $^{117}GVL^{119}$ motif was essential to this activity. Using a HEK-293T cell transfection system, we showed that the TnPrx1-CAT participated in the regulation of H_2O_2 and H_2O_2-dependent phosphorylation of p38 protein in cells. Additionally, CAT activity was also confirmed in human Prx1 (HsPrx1), suggesting that the Cys-independent Prx1-CAT activity is conserved from fish to mammals.

Experimental

Cloning and expression of recombinant Prx1 proteins

The open reading frames (ORFs) of *Prx1* genes from *T. nigroviridis* (*TnPrx1,* GenBank accession number: DQ003333) and *Homo sapiens* (*HsPrx1,* NM_001202431) were amplified by RT-PCR from mRNA isolated from pufferfish kidney and Hela cells, and cloned into pET28a or pMAL-c2E bacterial expression vector containing a His×6-tag or maltose-binding protein (MBP) at the N-terminus, as described [19,20]. TnPrx1 mutants were generated by site-directed mutagenesis by replacing all three Cys residues (i.e. Cys^{52}, Cys^{71} and Cys^{173}) with Ser residues to eliminate POX activity (denoted by POX$^-$CAT$^+$), or the $^{117}GVL^{119}$ motif with $^{117}HLW^{119}$ to suppress CAT-like activity (POX$^+$CAT$^-$), or both (POX$^-$CAT$^-$) (see Table 1 for details on the genotypes of constructs). Site-directed mutants of TnPrx1 were constructed using the overlapping extension PCR strategy. Taking the construction of POX$^+$CAT$^-$ as an example, two DNA fragments (named S1 and S2) were amplified by PCR using WT TnPrx1 ORF cDNA as the template and TnPrx1-EcoRI-F and TnPrx1-HLW-R or TnPrx1-HLW-F and TnPrx1-XhoI-R as the primer pair (see Table 2 for the description of primers). Then, the target POX$^+$CAT$^-$ encoding sequence was amplified using templates containing both S1

Table 1. Kinetic parameters of wild-type (WT) TnPrx1 and various mutants deficient in thioredoxin peroxidase (POX) and/or catalase (CAT)-like activities on H_2O_2 compared with those reported for mammalian glutathione peroxidases (GPxs) and CATs.

NS, Not suitable. All data are presented as the mean values ± standard deviations (SDs of each group).

Constructs	Genotype	DTT[1]	K_m or K' (μM)	k_{cat} (s^{-1})	$k_{cat}/K_m/$ ($\times 10^4$ M^{-1} s^{-1})	n^2
TnPrx1 (POX$^+$CAT$^+$)[3]	WT puffer fish Prx1	−	168 ± 8.8	1.8 ± 0.11	~1.0	4.7 ± 0.33
		+	214 ± 11.7 (Overall)	2.5 ± 0.36 (Overall)	~1.1 (Overall)	3.4 ± 0.34 (Overall)
			2.23 ± 0.03 (POX)	0.21 ± 0.01 (POX)	~8 (POX)	
TnPrx1 (POX$^-$CAT$^+$)	All 3 Cys → Ser	−	211 ± 7.1	2.3 ± 0.17	~1.1	3.7 ± 0.42
		+	227 ± 8.3	2.6 ± 0.26	~1.1	3.3 ± 0.46
TnPrx1 (POX$^+$CAT$^-$)	^{117}GVL → ^{117}HLW	−	~250	0.013 ± 0.002		
		+	4.15 ± 0.6	0.23 ± 0.01	~6	
TnPrx1 (POX$^-$CAT$^-$)	All 3 Cys → Ser and ^{117}GVL → ^{117}HLW	−	~250	0.016 ± 0.001		
		+	~250	0.016 ± 0.002		
HsPrx1 (WT)	WT human Prx1	−	347 ± 13.8	3.9 ± 0.16	~1.1	10.1 ± 1.8
		+	343 ± 11.2	4.0 ± 0.06	~1.1	8.8 ± 1.0
Mammalian GPx[4]	NS	NS	2×10^2–2×10^4	10^1–10^2	~10^4	
Mammalian catalase[4]	NS	NS	10^4–10^5	10^4–10^5	~10^2	

[1]Activity assayed with or without the reducing agent DTT (dithiothreitol, 100 μM). In the absence of DTT, only CAT-like activity plus a basal level of H_2O_2 consumption by oxidizing same molar amount of Cys residues in TnPrx1 and HsPrx1;
[2]n = Hill coefficient;
[3]Parameters in the presence of DTT were given for overall activity (i.e. POX + CAT) determined by allosteric sigmoidal model and for POX activity determined only by Michaelis–Menten model at the lower range of H_2O_2 concentrations (see curves in Figure 3a, inset);
[4]Data acquired from http://www.brenda-enzymes.org/.

Table 2. List of primers and their applications

Primer	Sequences (5′ to 3′)	Application
TnPrx1-EcoRI-F	GAATTCATGGCTGCAGGCAAAGCTC	Cloning (pET28)
TnPrx1-XhoI-R	CTCGAGGTGCTTGGAGAAGAACTCTTTG	Cloning (pET28)
TnPrx1-KpnI-F	GGGTACCGATGGATTACAAGGATGAC	Cloning (pMal)
TnPrx1-HindIII-R	CAAGCTTGGCTTAGTGCTTGGAGAAG	Cloning (pMal)
TnPrx1-Ser52F	CTTCACCTTTGTGTCCCCCACTGAAG	Mutation
TnPrx1-Ser52R	CTTCAGTGGGGGACACAAAGGTGAAG	Mutation
TnPrx1-Ser71F	CGGAAAATTGGATCCGAGGTCATCG	Mutation
TnPrx1-Ser71R	CGATGACCT CGGATCCAATTTTCCG	Mutation
TnPrx1-Ser173F	GCATGGAGAAGTTTCCCCTGCCGGC	Mutation
TnPrx1-Ser173R	GCCGGCAGGGGAAACTTCTCCATGC	Mutation
TnPrx1-HLW-F	CAATCTCTACAGACTACCACTTATGGAAGGAAGACGAAGG	Mutation
TnPrx1-HLW-R	CCTTCGTCTTCCTTCCATAAGTGGTAGTCTGTAGAGATTG	Mutation
HsPrx1-F	GCTGATAGGAAGATGTCTTCAGGAA	Cloning
HsPrx1-R	GCCAACTCAGGCCATTCCTACC	Cloning
HsPrx1-EcoRI-F	CCGGAATTCATGTCTTCAGGAAATGCTAAAATTG	Expression
HsPrx1-XhoI-R	CCGCTCGAGCTTCTGCTTGGAGAAATATTC	Expression
siRNA-402	GCACCAUUGCUCAGGAUUAUU	Gene silencing
siRNA-525	CCAGUUCACUGACAAACAUU	Gene silencing
siRNA-625	GCUCUGUGGAUGAGACUUUU	Gene silencing
siRNA-Ctrl	UUCUCCGAACGUGUCACGUU	Gene silencing control
TnPrx1-assay-F	TTTCCGGGAAATTGGA	qRT-PCR
TnPrx1-assay-R	AGATTGTGTGTCGTGT	qRT-PCR
HsPrx1-assay-F	CGCGTCTTGTTCTTGCCTGGTGTCG	qRT-PCR
HsPrx1-assay-R	CGCGTCTTGTTCTTGCCTGGTGTCG	qRT-PCR
Catalase-assay-F	TACCTGTGAACTGTCCCTACCGTGC	qRT-PCR
Catalase-assay-R	CATAGAATGCCCGCACCTGAGTAAC	qRT-PCR

and S2 and the primer pair TnPrx1-EcoRI-F and TnPrx1-XhoI-R. Typical PCR reactions were performed using Ex Taq™ Polymerase (TaKaRa) under the following conditions: 94°C for 5 min; 35 cycles of 94°C for 30 s, 55°C for 30 s, and 72°C for 1 min; and a final extension at 72°C for 10 min. All constructs were subjected to Sanger sequencing to verify the correctness of the gene sequences and desired mutations.

The expression of recombinant Prx1 proteins fused with His and MBP tags in *Escherichia coli* was performed at 37°C for 4 h after the addition of isopropyl β-D-1-thiogalactopyranoside (IPTG) (0.1 or 0.3 mM for His- or MBP-tagged proteins, respectively). Fusion proteins were purified from the soluble fractions by Ni-TNA agarose bead- or amylose resin-based affinity chromatography and eluted with elution buffer containing 250 mM imidazole (for His-tagged proteins) or 10 mM maltose (for MBP-tagged proteins) in accordance with the manufacturer's instructions (Novagen (pET28 system) and NEB (pMAL system)), or as specified [19,20]. Purified Prx1 proteins were subjected to SDS-PAGE analysis and stained with Coomassie Brilliant Blue. The protein purities were determined by densitometry using a 1D Image Analysis Software with Gel Logic 200 Imaging System (Eastman Kodak Co., USA).

A reversible monomer-to-dimer transition system was established to evaluate the Cys-dependent formation of dimers, in which the purified recombinant proteins in the form of monomers were first allowed to be oxidized to form dimers in air at 4°C, and then the resulting protein dimers were reduced to monomers by treating samples with 50 mM of DTT at room temperature for 10 min or as specified. The reduced and oxidized forms of Prx1 were detected by non-reducing SDS-PAGE. Prior to each activity assay, Prx1 proteins in the reduced form were subjected to extensive ultrafiltration with phosphate-buffered saline (PBS) to remove DTT.

Protein structure homology-modeling

TnPrx1 protein structure homology-modeling was performed using a rat Prx1 (PDB ID: 1QQ2; 80% amino acid identity to TnPrx1) as template. Global alignment of various structural models was performed by using PyMOL to produce various structural-model figures. The active site of TnPrx1 was predicted using an alpha-shape algorithm to determine potential active sites in the protein structures in MOE site finder. A pocket structure formed by conserved $^{117}GVL^{119}$ amino acid residues was predicted to be an H_2O_2-binding site. To test whether the GVL pocket was essential for the Prx1-CAT activity, we replaced $^{117}GVL^{119}$ with HLW residues containing large chains or aromatic rings to alter the pocket structure and abolish its ability to bind H_2O_2. The mutant was constructed by site-directed mutagenesis using overlapping extension PCR strategy as described above.

Enzyme activity assays

The reduction of H_2O_2 by TnPrx1 and HsPrx1 was determined by a modified sensitive Co(II catalysis luminol chemiluminescence assay as described [21]. Briefly, the luminol-buffer cocktail was composed by 100 µl of luminol (100 mg ml^{-1}) in borate buffer (0.05 M, pH 10.0) and 1 ml of Co(II) (2 mg/ml)-EDTA (10 mg ml^{-1}, pH 9.0). Reactions were started by mixing 50 µl of proteins (50 µg ml^{-1}) with 50 µl of H_2O_2 at concentrations between 0–500 µM for 1 min at 25°C, following by the addition of 1.1 ml of the luminol-buffer cocktail to stop the reaction. The same amount of PBS was used to substitute proteins in the control and for generating standard curves.

The intensity of emission was measured with an FB12 luminometer (Berthold Detection Systems, Pforzheim) and the maximum values were recorded. The kinetic parameters of Prx1 proteins were determined using the Michaelis-Menten and/or the allosteric sigmoidal kinetic models. The production of oxygen was measured with an oxygen electrode (#341003038/ 9513468), Mettler Toledo. The reaction was performed in 4 ml of 600 µM H_2O_2 solutions, and the measurement was started by the addition of proteins (POX$^+$CAT$^+$ dimers, 0.32 µM or POX$^-$CAT$^+$ monomers, 0.64 µM) under soft stirring. Oxygen production rates were monitored at specified time points. Reactions with bovine catalase (8 nM) (Sigma-Aldrich) and BSA (6 µM) were used as positive and negative controls, respectively.

Determination of enzyme properties

The effect of pH on Prx1-CAT activity was evaluated by detecting the reduction of H_2O_2 in reactions carried out in 0.2 mM Na_2HPO_4/0.1 mM citrate buffer at pH 2.0–8.0 and 50 mM disodium pyrophosphate/NaOH buffer at pH 8.0–11.0, respectively. The effect of temperature was tested between 0–70°C at pH 7.0. The thermal and pH stabilities were similarly assayed, except that concentrated Prx1 proteins were first treated at various temperatures for 1 h, or 6 h under different pH conditions, and then their specific activities were determined under regular assay conditions (i.e. pH 7.0 at room temperature).

Specific activities were also assayed for iron-saturated proteins prepared by mixing proteins with FeCl$_3$ (1:100 molar ratio), followed by ultrafiltration (MWCO = 10 kDa) to remove unbound iron. The role of iron in Prx1-CAT was further evaluated by iron chelation and rescue assays, in which TnPrx1 proteins were treated with 25 mM 4,5-dihydroxy-1,3-benzene disulfonic acid (tiron) and 50 mM 2,2′-dipyridyl (DP) at 4°C overnight, followed by ultrafiltration. Chelator-treated samples were then incubated with FeCl$_3$ (200 µM) or as specified at 4°C overnight, followed by ultrafiltration to remove unbound iron. The residual TnPrx1-CAT activities of iron-free and iron-rescued proteins were determined in standard reactions as described above. To confirm that iron was truly bound to TnPrx1, iron-rescued samples were subjected to extensive ultrafiltration with PBS, and the iron content was detected by the inductively coupled plasma optical emission spectroscopy (ICP-OES), Optima 8000DV, Perkin-Elmer, as described [22]. To evaluate whether the $^{117}GVL^{119}$ motif is involved in iron–binding, the pocket mutant (p.G117H/V118L/L119W) with the MBP tag was also subjected to iron content examination by ICP-OES.

The effects of seven other metals on the TnPrx1-CAT activity were also tested, in which WT TnPrx1 dimers were treated with tiron/DP mixture, and then reconstituted individually by incubating them with Mg^{2+}, Ca^{2+}, Cu^{2+}, Mn^{2+}, Co^{2+}, Ni^{2+} or Zn^{2+} (protein:metal molar ratio = 1:5) at 4°C overnight. The effects of two classic CAT inhibitors (DTT and 3-amino-1,2,4-triazole [3-AT]) on TnPrx1 were assayed by pretreating proteins with 10 mM 3-AT at 4°C overnight or 1 mM DTT at 25°C for 30 min. Bovine catalase was used as positive control. Enzyme activities were assayed as described above.

Knockdown of HsPrx1 by siRNA in HEK-293T cells

Three small interfering RNAs (siRNAs) targeting *HsPrx1* (siRNA-402, -525, and -562) and one negative control siRNA (siRNA-Ctrl) were synthesized by GenePharma (Shanghai, China) (Table 1). HEK-293T cells were cultured at 37°C in Dulbecco's modified Eagle's medium (DMEM, Invitrogen) supplemented with 10% fetal bovine serum (Gibco) in the presence of 5% CO_2. Transfection was performed using Polyethylenimine (PEI) in accordance with the manufacturer's recommended instructions (Sigma-Aldrich). Total RNA was isolated from HEK-293T cells transfected with siRNAs and/or TnPrx1 constructs using TRIzol reagent (Invitrogen). The levels of *HsPrx1* transcripts after transfections were monitored by qRT-PCR using SYBR *Premix Ex Taq*™ II kit (TaKaRa) and primers described in Table 2, in which the samples were first denatured at 95°C for 1 min, and then subjected to 40 cycles at 95°C for 10 s, 60°C for 30 s, and 72°C for 20 s. Each experimental condition included three biological replicates, and each biological sample included three technical replicates. The relative RNA expression was calculated using a $2^{-\Delta CT}$ method.

Effects of WT TnPrx1 and mutants on intracellular ROS level and the phosphorylation of P38 MAPK

The ORFs of WT and mutated *TnPrx1* genes were subcloned into pCMV-Tag2B vector. For transient transfection, WT or *HsPrx1*-silenced HEK-293T cells were plated in 100 mm culture plates (1.4×10^6 cells/plate), grown overnight, and transfected with 17 μg of WT Prx1 or mutant plasmids using Fugene reagent (Promega). Blank pCMV-Tag2B vector was used as negative control. After 48 h of post-transfection, cells were washed with PBS, and incubated with 2′7′-dichlorodihydrofluorescein diacetate (DCFH-DA, 200 μM, Sigma) in serum-free medium at 37°C for 30 min to allow uptake by cells and intracellular cleavage of the diacetate groups by thioesterase. Cells were washed with PBS to remove free DCFH-DA from the medium, and counted by trypan blue (0.4% exclusion method). Viable cells were then plated into collagen-coated 96-well plates (2×10^4 cells/well), and treated with H_2O_2 for 60 min at final concentrations of 0–850 μM or 0–800 μM for WT or *HsPrx1*-silenced HEK-293T cells, respectively. Intracellular fluorescence signals of oxidized DCFH at 0 and 1 h time points (T0 and T1) followed by the H_2O_2 treatment were measured with a Synergy H1 Hybrid Reader (BioTek, USA) ($\lambda_{ex}/\lambda_{em}$ = 485/525 nm). The relative fluorescence signal for each sample (RF_{sample}) was calculated using the following equations:

$$RF = \frac{\Delta F_{sample}}{\Delta F_{max}} \tag{1}$$

$$\Delta F_{sample} = \left(\frac{F_{(T1-T0)}}{F_{T0}}\right) \times 100\% \tag{2}$$

In order to evaluate the effect of TnPrx1 constructs on the phosphorylation of intracellular p38 MAPK, transfected cells treated with H_2O_2 (0–1200 μM or 0–800 μM for WT or *HsPrx1*-silenced cells) were collected and lysed. This was followed by Western blot analysis using antibodies against p38 (1:1000 dilution; Catalog No. 8690, Cell Signaling Technology, Danvers) and phosphorylated p38 protein (p-p38) (1:1000 dilution; Catalog No. 4511, Cell Signaling Technology, Danvers), respectively. The immuno-reactive bands were visualized using an enhanced chemiluminescence (ECL) system (Pierce, Rockford, IL).

Statistical analysis

All experiments were performed independently at least three times. Data were presented as the mean ± standard deviation of the mean (SD). Two-tailed Student's *t*-test was used to assess statistical significance between experimental and control groups.

Results

Cys-independent CAT-like activity in TnPrx1

Thioredoxin peroxidase (POX) was previously the only known enzyme activity in Prxs that relied on NADPH-dependent oxidoreduction between Trx and TrxR to maintain the continuation of their POX activity (Figure 1, Pathway II). In the absence of Trx/TrxR/NADPH cycle or a reducing agent (e.g. DTT), the reactions

stop after the formation of a C_P-C_R disulfide bound, in which one pair of Prx monomers may only reduce two H_2O_2 molecules. Four to six H_2O_2 molecules may be reduced when hyperoxidized without the formation of disulfide bonds (Figure 1, Pathway III).

Surprisingly, however, in the absence of a reducing agent, we observed that the recombinant WT TnPrx1 monomers (>99% purity) in reduced status were able to continuously reduce H_2O_2 molecules (Figure 2a–c), implying the presence of non-POX oxidoreduction activity in TnPrx1. Similar activity was observed when TnPrx1 was fully oxidized to form dimers (Figure 2b,d), confirming that the observed non-POX activity was independent of the status of Cys residues. The observed activity was not attributed to nonspecific background reactions as it was not observed in reactions containing no, or denatured, TnPrx1 (Figure 2c,d; first and last columns). Additionally, we also detected the O_2 production (Figure 2e,f), and the calculated ratio between the reduced H_2O_2 and the produced O_2 was 2.29:1, indicating that this activity was derived from a CAT-like activity (i.e. $2 H_2O_2 \rightarrow 2 H_2O + O_2$), rather than the POX activity that only produces H_2O.

To fully rule out the possibility that a trace amount of contaminating CAT from *E. coli* was present in the TnPrx1 preparations (despite >99% purity) and contributed to the activity, we prepared TnPrx1 proteins under different elution stringency (i.e. imidazole at 150–300 mM) to allow various impurities (i.e. containing various amounts of contaminants). We confirmed again that the activity was derived from TnPrx1, as it was correlated with the amount of TnPrx1, rather than with the level of impurity (Figure 2g,h).

The activity was iron-dependent, as it could be inhibited by ferrous/ferric chelators tiron and DP, and the addition of Fe^{3+} not only increased the activity of untreated TnPrx1, but also reversed the inhibition by chelators (Figures 2h and 3a). Fe^{3+} displayed low nanomolar-level binding affinity with TnPrx1 (apparent $K_d = 0.17$ μM), and a ~1:1 (metal:Prx1) stoichiometry (Figure 3c). To confirm the iron-TnPrx1 binding, we directly evaluated the iron content of recombinant TnPrx1 proteins under various conditions. Proteins were subjected to extensive ultrafiltration to remove unbound iron. The molecular ratio between iron and untreated TnPrx1 protein was 0.64 (±0.002):1 (Figure 3d). Treatment by chelators reduced the ratio to 0.08 (±0.003):1, whereas the addition of $FeCl_3$ (200 μM) restored the ratio to 0.75 (±0.006):1 (Figure 3d). These observations indicated that each TnPrx1 binds to one iron, and up to 75% of the recombinant TnPrx1 proteins were in their active form.

Additionally, the effect of other metals, including Mg^{2+}, Ca^{2+}, Cu^{2+}, Mn^{2+}, Co^{2+}, Ni^{2+} and Zn^{2+} on the CAT-like activity was tested, but no enhancement activity was observed (data not shown). The dependence on iron, but not on reducing agents and Cys residues were characteristic to CATs, further confirming that the observed activity was not derived from the POX activity of Prxs. Instead, it resembled a CAT that was previously unknown to Prxs. However, TnPrx1 was insensitive to the inhibitors of typical CATs, such as DTT and the irreversible inhibitor 3-AT (Figure 3e,f), suggesting that Prx1 might represent a new class of CAT-like enzyme. Indeed, unlike typical CATs, TnPrx1 lacked the Soret absorbance peak unique to heme-containing moieties (data not shown), indicating that it is a heme-less metalloprotein, rather than a heme-containing protein.

In the presence of DTT, WT TnPrx1 displayed Michaelis-Menten kinetics on low concentrations of H_2O_2 (i.e. <100 μM) (Figure 4a). The K_m value was 2.2 μM, which was comparable to the K_m values previously reported for Prx1-POX activities that were typically much lower than 20 μM [7]. At higher H_2O_2 concentrations (>50 μM), TnPrx1 exhibited allosteric kinetics, suggesting a positive cooperativity, i.e. $K'_{app} = 214$ μM and Hill coefficient (n) = 3.4. This result implies that reducing Prx1 has a relatively low affinity for O_2. However, binding of one H_2O_2 to Prx1 might change the structure of the binding site, which allows the second H_2O_2 to bind more easily or the bounded H_2O_2 to be catalyzed by iron more rapidly, thereby increasing O_2 affinity. In the absence of DTT, however, TnPrx1 showed little or no activity until [H_2O_2] reached >50 μM ($K'_{app} = 168$ μM, $n = 4.7$) (Figure 4a; Table 1). The data were in agreement with the notion that TnPrx1 possessed both POX and CAT activities, since the activities with DTT (POX + CAT) were higher than those without DTT (CAT only) by a relatively constant rate (i.e. 2.5 s^{-1}), determined by a 'Michaelis-Menten + allosteric sigmoidal' model.

Since CAT activity was described for the first time in a Prx1 of fish origin, we wanted to know whether it was also present in mammalian Prx1. We expressed recombinant human Prx1 (HsPrx1) and performed a similar assay with and without a reducing agent. Our data supported the contention that HsPrx1 was also bifunctional, since it possessed POX and CAT activities with kinetic parameters comparable to those of TnPrx1 (i.e. $K'_{app(-DTT)} = 347$ μM, $n_{(-DTT)} = 10.1$, $K'_{app(+DTT)} = 342$ μM, and $n_{(+DTT)} = 8.8$, respectively) (Figure 4e;
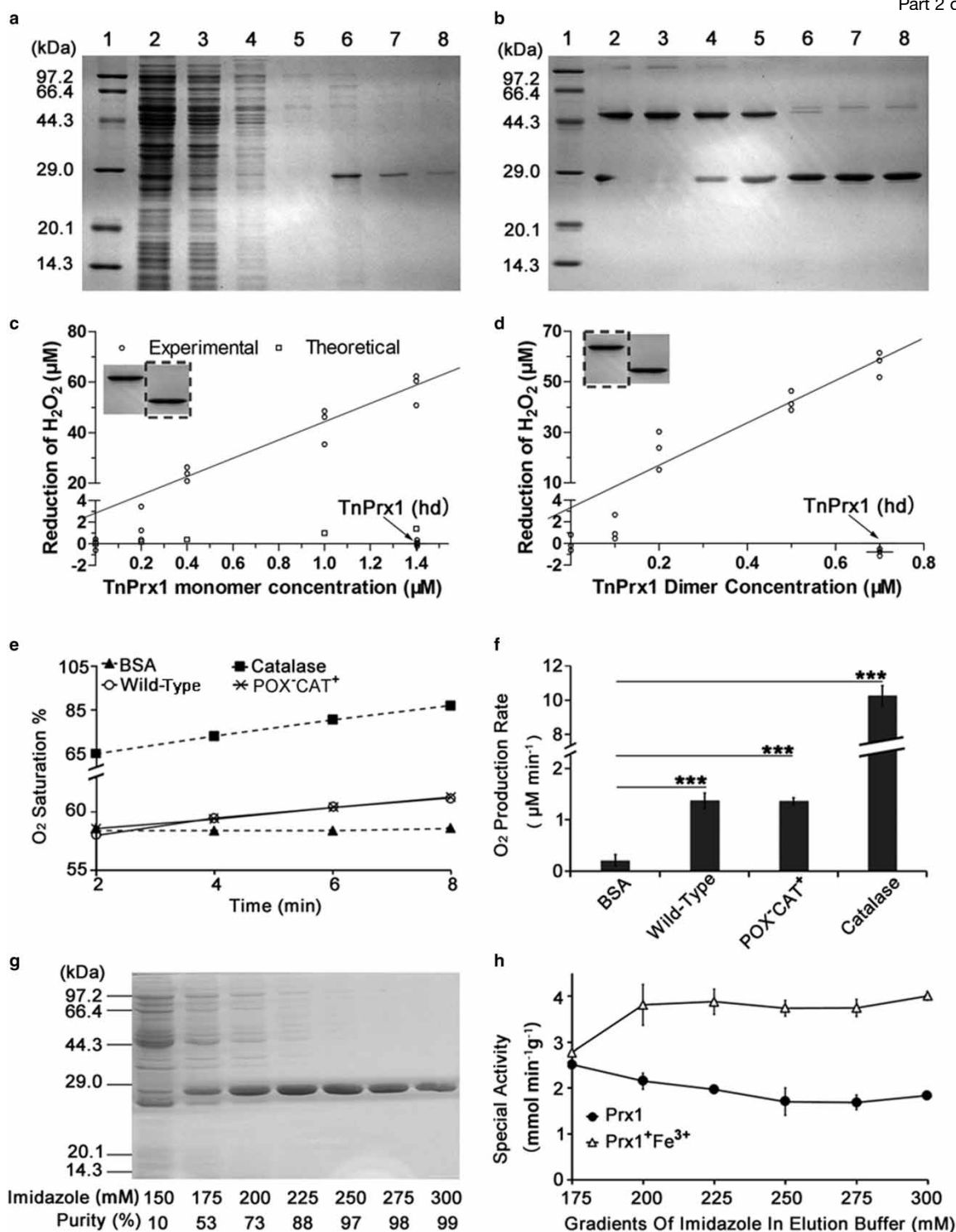
Figure 2. Verification of the catalase (CAT)-like activity of TnPrx1 and mutants. Part 1 of 2

(**a**) Expression and purification of soluble TnPrx1 protein. Lanes: 1, protein markers; 2, crude cell lysate; 3, flow-through; 4–5, 40 mM imidazole wash; 6–8, eluted recombinant protein (250 mM imidazole); (**b**) Reductive dissociation of TnPrx1 dimer induced by DTT. Lanes: 1, protein markers; 2–8, proteins treated with different concentrations of DTT (dithiothreitol) (0, 0.1, 0.5, 1, 5, 10 and 50 mM); (**c,d**) Activities of TnPrx1 in monomers (**c**) and dimers (**d**) in the absence of a reducing agent by detecting the reduction of H_2O_2 using a luminol chemiluminescence assay after incubation with 300 μM H_2O_2 for 10 min at

PORTLAND
PRESS

Figure 2. Verification of the catalase (CAT)-like activity of TnPrx1 and mutants. Part 2 of 2

25°C. The bands in the dashed box denote the TnPrx1 monomers and dimers used in the corresponding assays. Theoretical values represented the maximal reduction of H_2O_2 possibly achieved by the oxidation of three TnPrx1 Cys residues in a given amount of TnPrx1 protein in the absence of reductants or redox recycling. hd = heated denatured TnPrx1 protein (at 100°C for 10 min); (**e,f**) Detection of O_2 production in reactions containing H_2O_2 and various protein constructs (i.e. 0.32 μM wild-type dimers, 0.64 μM POX$^-$CAT$^+$ monomers, 8 nM catalase and 6 μM BSA) with oxygen electrode technique; POX = Cys-dependent thioredoxin peroxidase; (**g,h**) Gradient elution of TnPrx1 protein with varied concentrations of imidazole in elution buffer (**g**), and their corresponding activity by measuring the reduction of H_2O_2 with or without the addition of extra iron (200 μM) by luminol chemiluminescence (**h**). TnPrx1 concentration was determined by thin-layer gel optical scanning. Activity was normalized to mmol of H_2O_2 reduced per min per gram of TnPrx1 protein. Data are representative of at least three independent experiments. The error bars represent standard deviations (SDs), and statistical significances between experimental and control groups were determined by Student's t-test. ***$P < 0.001$.

Table 1). Although Prxs from more species need to be examined to make a firm conclusion, the data here suggest that the CAT-like activity is probably conserved among vertebrate Prx1 from fish to mammals.

To further validate TnPrx1-CAT activity, we performed a site-directed mutagenesis and constructed a mutant by replacing all three Cys residues with Ser residues to completely eliminate its Cys-dependent POX activity. The resulting mutant (POX$^-$CAT$^+$) was unable to form dimers as expected (Figure 4g,h), but was still capable of converting H_2O_2 to O_2 (Figure 2e,f). The POX$^-$CAT$^+$ mutant displayed virtually identical sigmoidal curves when assayed with and without DTT, which resembled those of WT TnPrx1 without DTT and those of similar kinetic parameters (i.e. $K'_{app(-DTT)} = 211$ μM, $n_{(-DTT)} = 3.7$, $K'_{app(+DTT)} = 227$ μM, and $n_{(+DTT)} = 3.3$), respectively (Figure 4b; Table 1). These observations confirmed that the observed TnPrx1-CAT activity was truly independent of the Cys residues and the reducing agent.

Potential active site for the CAT-like activity in TnPrx1

The discovery of a previously unknown Prx1-CAT activity prompted us to search for the functional motif. By examining a previously reported structure of rat Prx1 (PDB ID: 1QQ2), and homology-based modeling of TnPrx1, we observed a flexible loop consisting of six residues, Gly^{117}, Val^{118}, Leu^{119}, Phe^{127} (rat Prx1) or Tyr^{127} (TnPrx1), Ile^{142} and Ile^{144} at the dimer interface, in which a H_2O_2 molecule could well fit into a pocket formed by the highly conserved ^{117}GVL^{119} residues (Figure 5). To test whether this pocket might contribute to the TnPrx1-CAT activity, we generated a TnPrx1 construct by replacing ^{117}GVL^{119} with ^{117}HLW^{119} (denoted by POX$^+$CAT$^-$) to alter the pocket structure (Figure 4f). Indeed, the mutant POX$^+$CAT$^-$ lost CAT-like activity (i.e. no activity without DTT in the reactions), but retained only DTT-dependent POX activity, which followed Michaelis-Menten kinetics that were characteristic to Prx1-POX activity ($K_m = 4.15$ μM) (Figure 4c; Table 1).

To further dissect individual TnPrx1-POX and Prx1-CAT activities, we generated a double-mutation (POX$^-$CAT$^-$), in which all Cys residues and ^{117}GVL^{119} were replaced by Ser and ^{117}HLW^{119}, respectively. As expected, this double-negative mutant lost both POX and CAT activities and was unable to reduce H_2O_2 regardless of whether DTT was present or not (Figure 4d). Among all the mutants tested, POX$^-$CAT$^+$ also displayed expected iron-dependency, in which iron chelators inhibited its activity that could be restored by adding iron (Figure 3b), whereas the two CAT$^-$ mutants (i.e. POX$^+$CAT$^-$ and POX$^-$CAT$^-$) only retained low activity (6% vs. WT) that were unaffected by iron chelators and iron (data not shown). Moreover, the molecular ratio between iron and TnPrx1 protein of the two CAT$^-$ mutants remained approximately 1:1 (i.e. iron:POX$^+$CAT$^-$ = 0.93 (±0.005):1; iron:POX$^-$CAT$^-$ = 0.80 (±0.002):1), which was not significantly different from that between iron and WT TnPrx1 ($P = 0.09$ and $P = 0.14$, respectively). This result suggests that the replacement of ^{117}GVL^{119} by ^{117}HLW^{119} merely destroyed the substrate binding site but not the iron binding site (Supplementary Figure S1). Additionally, the TnPrx1-CAT activity tolerated low temperature more than pH, as it was able to retain virtually constant peak activity between 0–40°C, but only retained peak activity at ~pH 7.0 (Figure 6).

Collectively, these observations confirm that TnPrx1 possesses both POX and CAT activities, and the residues ^{117}GVL^{119} are critical to Prx1-CAT activity. TnPrx1-POX acted on H_2O_2 with much higher affinity ($K_m = 4.15$ μM), but had a relatively low maximal activity ($k_{cat} = 0.23$ s^{-1}) with a wider range of H_2O_2 levels (Table 1; Figure 4c); whereas Prx1-CAT acted on H_2O_2 with lower affinity ($K'_{(-DTT)} = 210.7$ μM), but had a much higher activity ($k_{cat} = 2.3$ s^{-1}) (Table 1).
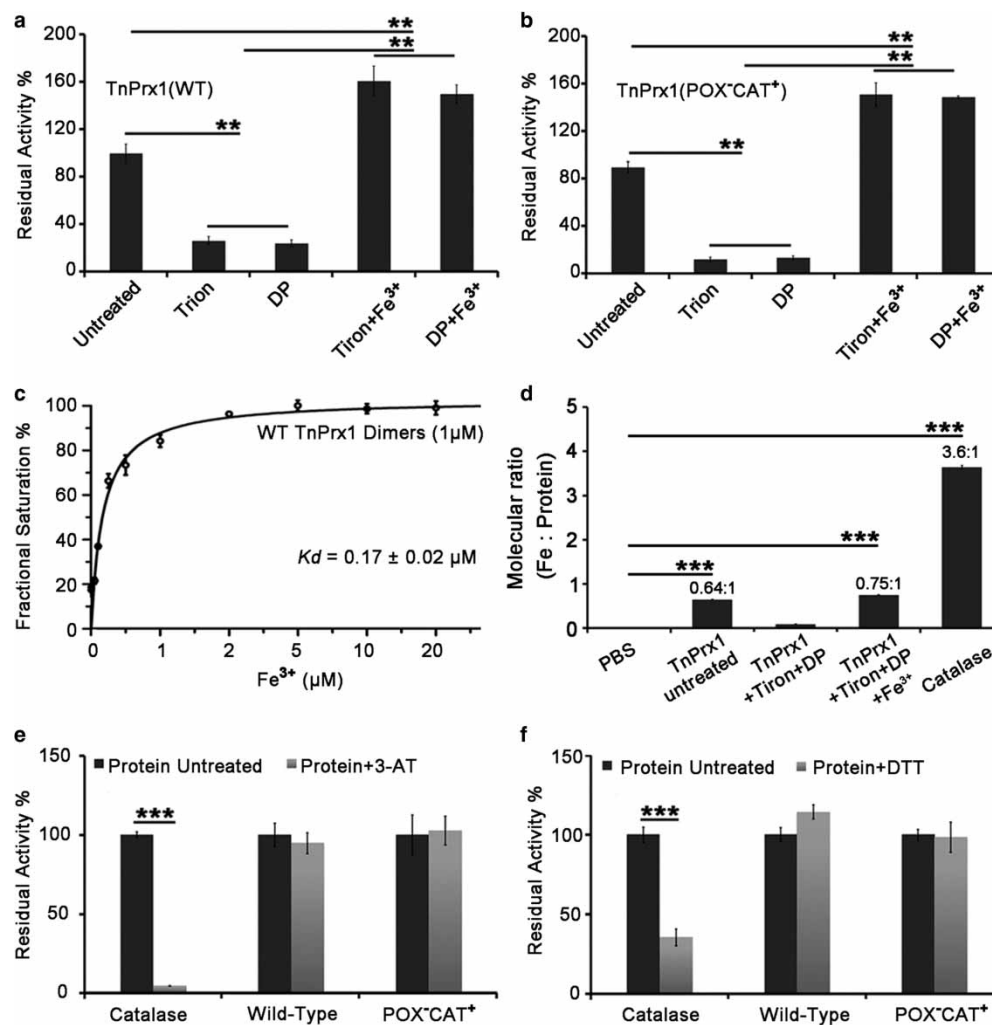
Figure 3. Iron-dependency and inhibition of TnPrx1 and mutants determined by measuring the reduction of H_2O_2.

(**a,b**) Effects of iron chelators (25 mM 4,5-dihydroxy-1,3-benzene disulfonic acid [tiron] and 50 mM 2,2′-dipyridyl [DP]) on the CAT activity of wild-type (WT) TnPrx1 and mutants, and restoration of the activity by the addition of Fe^{3+} (200 μM). Residual activities were expressed as the percentage activity (vs. untreated WT TnPrx1); (**c**) Dose-dependent WT TnPrx1 activity on Fe^{3+}. Residual activities were expressed as the percentage activity (vs. WT TnPrx1 treated with 200 μM Fe^{3+}); (**d**) The molar ratio between TnPrx1 protein and bound iron determined by ICP-OES (inductively coupled plasma optical emission spectroscopy). TnPrx1 was treated as specified, followed by extensive washes with water by ultrafiltration prior to ICP. Bovine catalase and PBS were used as controls; (**e,f**) Effects of catalase inhibitors 3-Amino-1,2,4-triazole (3-AT) and dithiothreitol (DTT) on the CAT activity of WT TnPrx1 and mutants. CAT was used as positive control. Protein samples (50 μl, 50 μg ml^{-1}, pretreated with 3-AT or DTT) were reacted with 50 μl of H_2O_2 solutions (300 μM) for 1 min. The residual activities were measured by luminol chemiluminescence assay and expressed as the percent activity (vs. untreated WT TnPrx1). Data are representative of at least three independent experiments. The error bars represent standard deviations (SDs), and statistical significances between experimental and control groups were determined by Student's t-test. $**P < 0.01$, $***P < 0.001$. CAT = Catalase-like activity of peroxiredoxin 1.

Implication of TnPrx1-CAT in regulating ROS level and signaling

The physiological roles of TnPrx1-CAT activity were investigated using a mammalian cell transfection system. First, we transfected HEK-293T cells to overexpress various TnPrx1 constructs, and examined the effects in regulating intracellular ROS (iROS) in response to H_2O_2 treatment. The expression of TnPrx1 constructs was confirmed by qRT-PCR (Figure 7a,b). We observed a general trend that cells overexpressing CAT$^+$ proteins (i.e. WT and POX$^-$CAT$^+$) had lower iROS levels than those expressing CAT$^-$ proteins (i.e. blank vector,
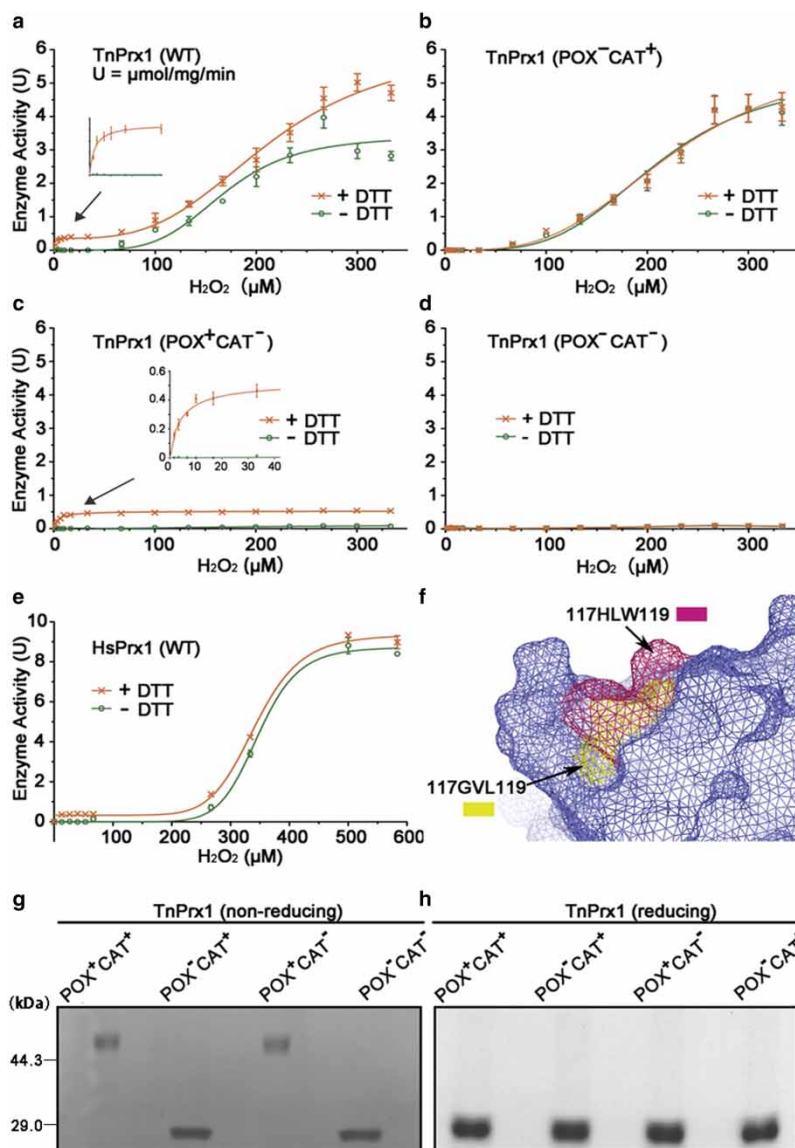
Figure 4. Kinetic features of Prx1 proteins.

(**a–e**) Enzyme kinetics curves for wild-type (WT) and mutated pufferfish Prx1 (TnPrx1) and WT human Prx1 (HsPrx1) with or without DTT (dithiothreitol). (**f**) Structural comparison of the potential cavity of WT Prx1 protein (yellow) and its mutant (warm pink) in mesh form. The image is a merged model of the two Prx1 proteins; (**g,h**) The dimeric versus monomeric status of TnPrx1 proteins in non-reducing or reducing SDS-PAGE (Sodium dodecyl sulfate-Polyacrylamide Gel Electrophoresis), respectively. All TnPrx1 proteins were treated with monomer-to-dimer transition protocol prior to the assays.

POX$^+$CAT$^-$ and POX$^-$CAT$^-$) in response to the treatment of 150–600 μM exogenous H$_2$O$_2$ (Figure 7c). The iROS levels were significantly downregulated in cells overexpressing CAT$^+$ proteins compared with the control cells (transfected with blank vector) at exogenous H$_2$O$_2$ concentrations between 150 and 400 μM (Figure 7c; $P < 0.05$ or $P < 0.001$). However, no significant differences were observed in those expressing CAT$^-$ proteins in response to 150–400 μM exogenous H$_2$O$_2$ treatment (Figure 7c,d).

Second, since H$_2$O$_2$ was known to also function as a signaling molecule, particularly in regulating kinase-driven pathways [23], we tested whether Prx1-CAT-associated regulation of intracellular H$_2$O$_2$ affected the phosphorylation of p38 protein that played a central role in the p38 mitogen-activated protein kinase (MAPK) signaling pathway. In HEK-293T cells transfected with blank or double-negative (POX$^-$CAT$^-$) plasmids, there
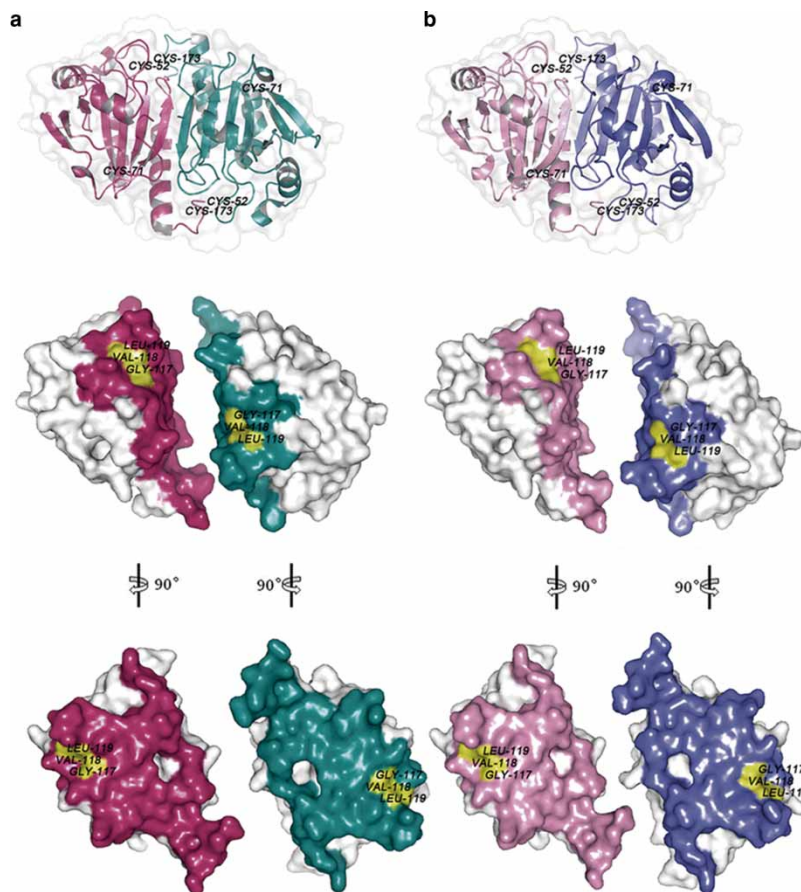
Figure 5. Structural comparison between rat Prx1 (PDB ID:1QQ2) (a) and TnPrx1 determined by homology-modelling (b).
Structural models were represented in surface forms prepared using PyMOL software (www.pymol.org). The amino acids located at the dimer interface are shown in colors. The pockets containing the ^{117}GVL^{119} motif in rat Prx1 and TnPrx1 are highlighted in yellow.

were low background levels of phosphorylated p38 (p-p38) in the absence of H_2O_2 stimulation (0 μM) (Figure 8). The levels of p-p38 in cells treated with 225–1200 μM H_2O_2 displayed a bell-curve that peaked in the 525–900 μM H_2O_2 groups, which was comparable to previously reported data [24]. When CAT$^+$ constructs (i.e. WT and POX$^-$CAT$^+$) were overexpressed, a considerable delay of phosphorylation of p38 was observed, as p-p38 was significantly ($P < 0.05$) up-regulated in cells challenged with H_2O_2, starting at 525 μM, peaked in the 900–1200 μM.

On the other hand, in cells overexpressing POX$^+$CAT$^-$ TnPrx1, no significant delay of p38 phosphorylation was observed, as p-p38 was only significantly up-regulated in cells challenged with H_2O_2; this started at 375 μM, peaked at approximately 750 μM and declined at 1200 μM (Figure 8), with a pattern was similar to that of the blank or double-negative group. Although further studies are needed to fully dissect the physiological roles of individual Prx1-POX and Prx1-CAT activities in cells and *in vivo*, these observations provide primary evidence on the involvement of the TnPrx1-CAT activity in regulating ROS-mediated p38 signaling pathway when cells were incubated with high micromolar to low millimolar level of H_2O_2.

We also employed an siRNA-silencing technology to minimize the effect of endogenous HsPrx1 in assaying the activity of *TnPrx1* constructs on iROS and the phosphorylation of p38. Among the three siRNA constructs, siRNA-402 showed the highest efficacy in silencing *HsPrx1* (i.e. ~94% with siRNA-402 vs. 81–83% with siRNA-525 and siRNA-562) (Figure 9a). Thus, siRNA-402 was used for subsequent functional investigations. Various *TnPrx1* constructs were co-transfected with siRNA-402 into HEK-293T cells. iROS and p-p38 levels were measured in WT and *HsPrx1*-silenced cells after H_2O_2 treatment (Figure 9b). Results showed that the iROS levels
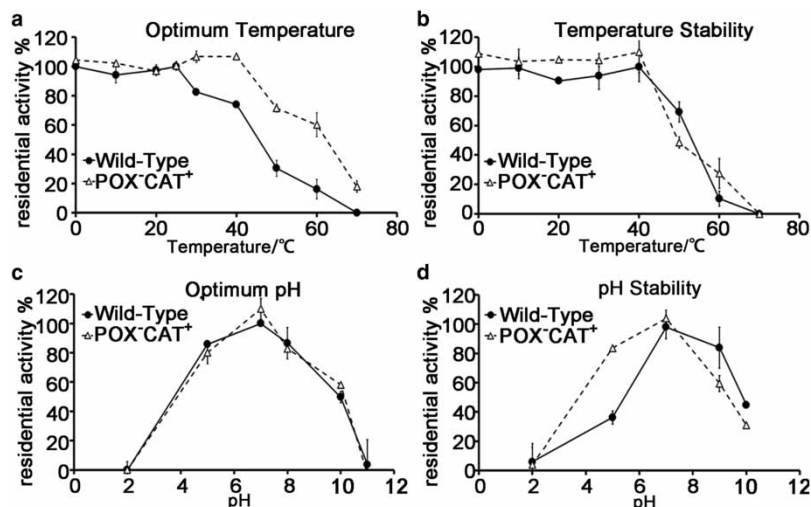
Figure 6. The effect of pH and temperature on catalase (CAT)-like activity and the stability of TnPrx1 proteins.
(**a**) The effect of temperature on residual Prx1-CAT activity. The activity assay was performed at pH 7.0 and at various temperatures. (**b**) The effect of temperature on Prx1-CAT stability. All the proteins were incubated at pH 7.0 and at various temperatures for 1 h and then the residual activity was estimated. (**c**) The effect of pH on residual Prx1-CAT activity. The activity assay was performed at room temperature and at various pH values. (**d**) The effect of pH on Prx1-CAT stability. The proteins were incubated with various pH at 4°C for 6 h and then the residual activity was measured.

in cells transfected with CAT^+ constructs (i.e. WT and POX^-CAT^+) were significantly lower than those transfected with CAT^- constructs (i.e. blank vector, POX^+CAT^-, and POX^-CAT^-) in response to the treatment of H_2O_2 at 100–600 μM (Figure 9c; $P < 0.05$, or $P < 0.01$). Similarly, a considerable delay of p38 phosphorylation upon H_2O_2 stimulation was observed in cells expressing CAT^+ TnPrx1 proteins compared with those expressing CAT^- proteins; the peak point for significant upregulation of p-p38 was shifted from 600 μM in cells expressing CAT^- TnPrx1 proteins to 800 μM in cells expressing CAT^+ TnPrx1 proteins (Figure 10; ($P < 0.05$ or $P < 0.01$). These observations were consistent with the results using WT HEK-293T cells (Figures 7 and 8), further supporting the functional role of TnPrx1-CAT activity in regulating iROS level and signaling.

Discussion

Eukaryotic cells contain a complex system to detoxify and regulate H_2O_2 and other reactive oxygen species. These include small molecules, such as ascorbic acid, β-carotene, glutathione, and α-tocopherol, and various enzymes, such as superoxide dismutase (SOD), catalase (CAT), glutathione peroxidase (GPx) and peroxiredoxin (Prx) [25]. Some of these enzymes or isoforms are mainly cytosolic (e.g. Prx1, Prx2, Prx5, Prx6, SOD1 and GPx1), while others may be compartmentalized (e.g. catalase in peroxisome, SOD2 and Prx3 in mitochondria, SOD3, GPx3 and Prx4 in extracellular region), which constitutes a precise antioxidant network for the defense against various oxidative stresses in the diverse cellular activities [4,26,27].

Cells are known to rely heavily on Prxs in scavenging H_2O_2 and other ROS molecules. In fact, they are the third most abundant proteins in erythrocytes, or represent 0.1–1% of total soluble proteins in other cells [4,7,26,28,29], and Prx1/2-knockout in mice might lead to the development of severe blood cell diseases (e.g. hemolytic anemia and hematopoietic cancer) [30,31]. Prxs are widely distributed and have been found in animals, plants, fungi, protists, bacteria and cyanobacteria, suggesting that they are a family of ancient proteins essential to a variety of critical cellular activities [32,33].

Prxs were previously recognized only as a family of thioredoxin POX, for which the biochemical features and biological functions were subjected to extensive investigations [23]. In the present study, we discovered that TnPrx1 and HsPrx1 are bifunctional and possess both Cys-dependent POX and Cys-independent CAT-like activities, which further extends our understanding of this important family of antioxidant proteins. The CAT-like activity in TnPrx1 was validated by the identification of the active site containing the GVL motif, which also enabled us to generate mutants lacking CAT and/or POX activity for dissecting their individual activities. Our
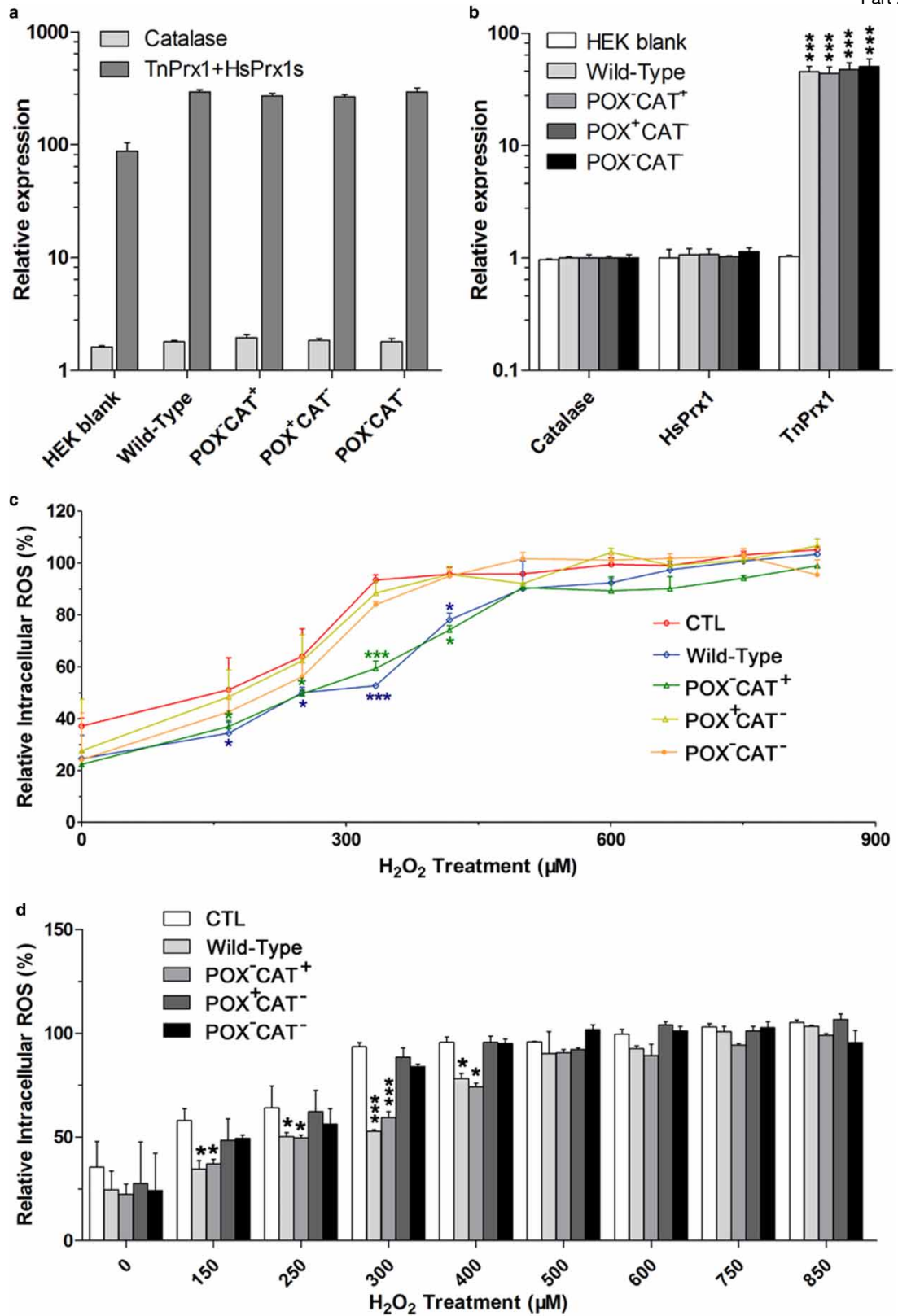
Figure 7. Involvement of TnPrx1 constructs in regulating intracellular ROS (iROS) in HEK-293T cells. Part 1 of 2

(**a,b**) The expression of various TnPrx1 constructs in transfected cells were confirmed by qRT-PCR (real-time quantitative

PORTLAND PRESS

Figure 7. Involvement of TnPrx1 constructs in regulating intracellular ROS (iROS) in HEK-293T cells.   Part 2 of 2

polymerase chain reaction) compared with those of endogenous HsPrx1 and catalase (CAT) genes. The relative levels of Prx1 transcripts (HsPrx1) only in blank control, or HsPrx1 + TnPrx1 in transfected cells were determined using a pair of primers derived from regions conserved between fish and mammalian Prx1 genes (Table 2). (**a**) Fold changes of Prx1 and catalase transcripts were expressed relative to the catalase transcripts in the blank control. (**b**) Fold changes of HsPrx1 and TnPrx1 transcripts were expressed relative to the transcripts of their own genes in the blank control. (**c,d**) Effects of TnPrx1 constructs on intracellular ROS in transfected cells treated with exogenous H_2O_2 as determined by DCFH (dichlorodihydrofluorescein diacetate) fluorescence assay. Cells transfected with blank vector were used as the negative control. The error bars represent standard deviations (SDs), and statistical significances between experimental and control groups were determined by Student's t-test. $*P < 0.05$, $***P < 0.001$.

data suggested that previously observed antioxidant activity in WT Prx1 (at least in some animals) were in fact a combined activity of Prx1-POX and Prx1-CAT. The alternation of GVL motif abolished TnPrx1-CAT activity, but not TnPrx1-POX activity (Figure 4c, Table 1). This suggests that Prx1 contained two independent H_2O_2 binding sites, which is in agreement with previous reports that the H_2O_2-binding site for the Cys-dependent POX activity was near the Cys^{51} and Cys^{172} residues but distant from the GVL site [34–36]. In fact, Prx1 was identified as early as the 1990s. However, the CAT activity of this protein has never been reported. This shortfall might be due to the limitations of the sensitive H_2O_2-detection method previously available and the universal usage of NADPH-dependent examination on Prx1 activity in early investigations. The latter of which was suitable for the determination of Prx1-POX activity (but not CAT activity), which was reflected indirectly by the consumption of NADPH. In addition, the concentration of H_2O_2 used in previous Prx1-POX studies was rather low because of the high affinity of Prx1-POX to H_2O_2 but the limited hydrolysis capacity for H_2O_2 (<20 μM). The underlying substrate (H_2O_2) concentration is extremely low for detection considering the CAT activity.

CATs are heme-containing enzymes [37]. Mammalian Prx1 was previously identified as a heme-binding protein 23 kDa (HBP23) [10,38], and a bacterial 2-Cys peroxiredoxin alkyl hydroperoxide reductase C (AhpC) was also reported to be able to bind heme [39], although heme-binding is non-essential to their functions. Our data indicated that TnPrx1-CAT activity was not heme-related, but rather was dependent on mononuclear iron. However, the exact iron-binding site remains to be determined. Sequence analysis indicates that Prx1 proteins from *T. nigroviridis* and mammals contain a 2-His-1-carboxylate facial triad-like motif (e.g. motif $^{81}HX_2HX_{36}E^{121}$ in TnPrx1) that is conserved in mononuclear non-heme iron enzymes [40]. Additionally, a Trp^{87} residue is also present at the motif. Aromatic residues, particularly Trp and Tyr, are known to be enriched at the Fe-sites of iron-proteins [41]. The involvement of aromatic residues in redox catalysis and/or electron transfer is not yet fully understood, but their capability to mediate electron transfer reactions makes them most suitable for tunneling electrons to/from redox sites [41]. On the other hand, the putative facial triad is not in the immediate proximity of the GVL motif. Therefore, its involvement in iron-binding and the mechanism of iron-mediated electron transfer for the Prx1-CAT activity need to be verified by further structure-based analysis.

Previous studies showed the existence of non-heme catalases in lactic acid bacteria, such as *Pedicoccus cerevisiae* and *Lactobacillus plantarum*, which are dependent on non-heme manganese [42,43]. A recent study has reported that a non-heme iron(III) CAT mimic, the complexes of 14-membered tetraaza macrocycles, can catalytically decompose H_2O_2 to H_2O and O_2, similarly to the native CAT enzyme [44]. Moreover, other non-heme iron binding proteins, such as phenylalanine hydroxylase, isopenicillin N synthase and anthocyanidin synthase, were identified from *Rattus norvegicus*, *Aspergillus nidulans*, and *Streptomyces clavuligerus*, respectively [40]. However, a native non-heme iron catalase has not been reported yet in any vertebrates and other organisms. To the best of our knowledge, the present study is the first to report a native non-heme iron catalase-like enzyme in vertebrate species, adding a new member to the CAT superfamily.

The sequence identity and similarity of vertebrate Prx1 are over 77% and 88% (Table 3) respectively, and the active site of CAT activity is completely conserved among Prx1 proteins, suggesting that CAT activity may be a ubiquitous function of Prx1 family members. The confirmation of reductant-independent HsPrx1-CAT activity indicates that this new function is probably conserved, at least in some vertebrates. Furthermore, $^{117}GVL^{119}$ are conserved in Prx1–3, while $^{117}GVY^{119}$ are conserved in Prx4. Although the Prx5 and Prx6 share low similarity with Prx1–4, they have similar 3D structures [45], suggesting that CAT activity might be present in other Prxs, at least Prx1–3. It might also explain why some parasites and cyanobacteria do not contain CAT and GPx, but have diverse Prx homologies [32,46].
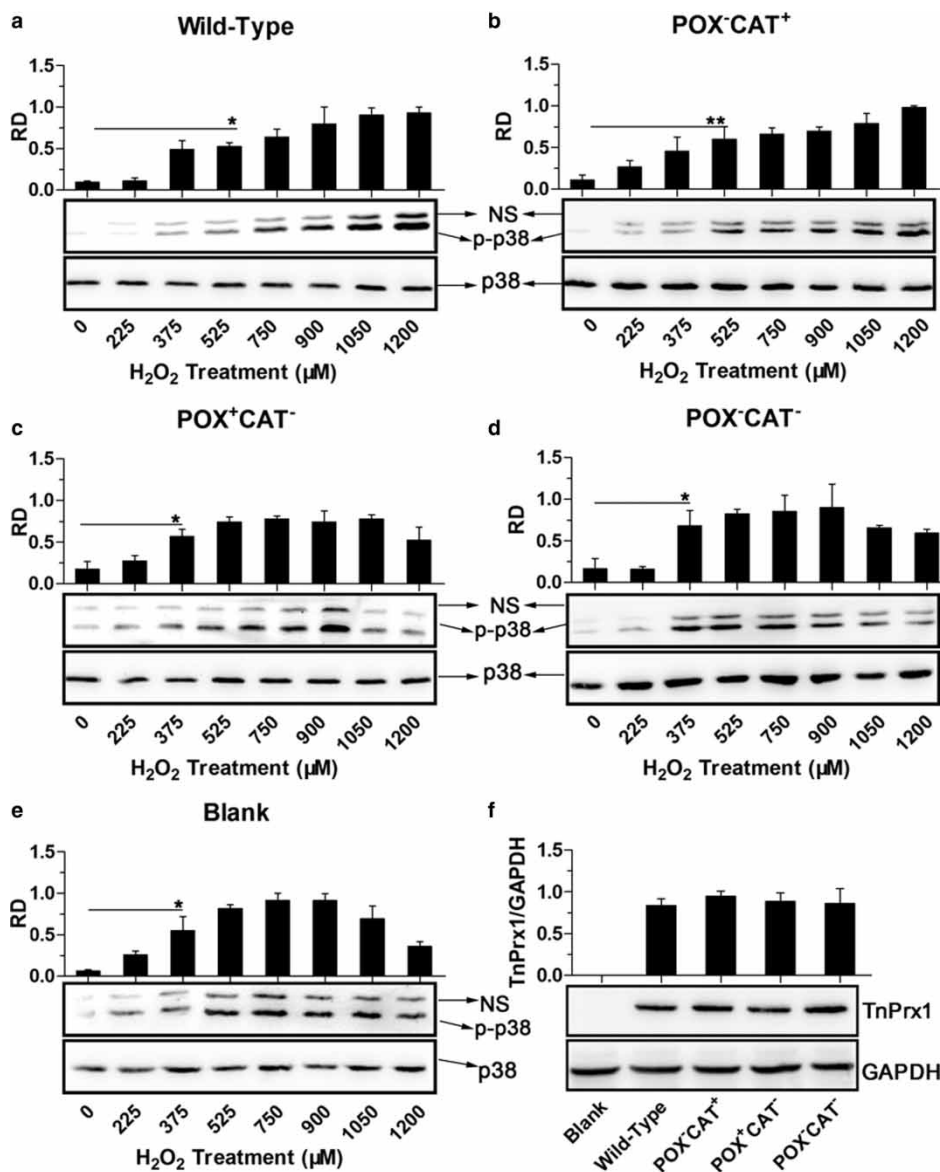
Figure 8. Effects of various TnPrx1 constructs on ROS-mediated phosphorylation of p38 MAPK in HEK-293T cells.
(**a–e**) Western blot analysis was conducted on total protein extracts from cells transfected with various TnPrx1 constructs and treated with various concentrations of exogenous H_2O_2 using antibodies specific to p38 and phosphorylated p38 (p-p38), respectively. Blank control cells received no transfection. Representative data from one of the three or more independent experiments were shown. Note: Antibody to p38 recognized a single band at 43 kDa, while antibody to p-p38 also produced a nonspecific band (NS) above the major band at 43 kDa for each sample. The NS bands were much weaker than—but proportional to—the major bands, a finding that was also observed by other investigators (e.g. [55–57]). Bar charts showed relative density (RD) of p-p38 major bands (vs. p38). The error bars represented standard deviations (SDs) from three replicated blots. An asterisk in each bar chart indicates the lowest concentration of exogenous H_2O_2 starting to give statistical significance between H_2O_2-treated and untreated controls (*$P < 0.05$ by Student's t-test); (**f**) Confirmation on the protein expression from TnPrx1 constructs by Western blot analysis using antibodies specific to His-tag and to human GAPDH control, respectively. RD = relative density; POX = Cys-dependent thioredoxin peroxidase; CAT = Catalase-like activity of peroxiredoxin 1.

The intracellular concentrations of H_2O_2 and other ROS molecules *in vivo* are not precisely known, but may range from sub- to lower micromolar levels in various prokaryotic and eukaryotic cells. However, intracellular H_2O_2 levels may rise to the order of 100 μM in phagocytes, and the transient H_2O_2 levels may reach >200 μM
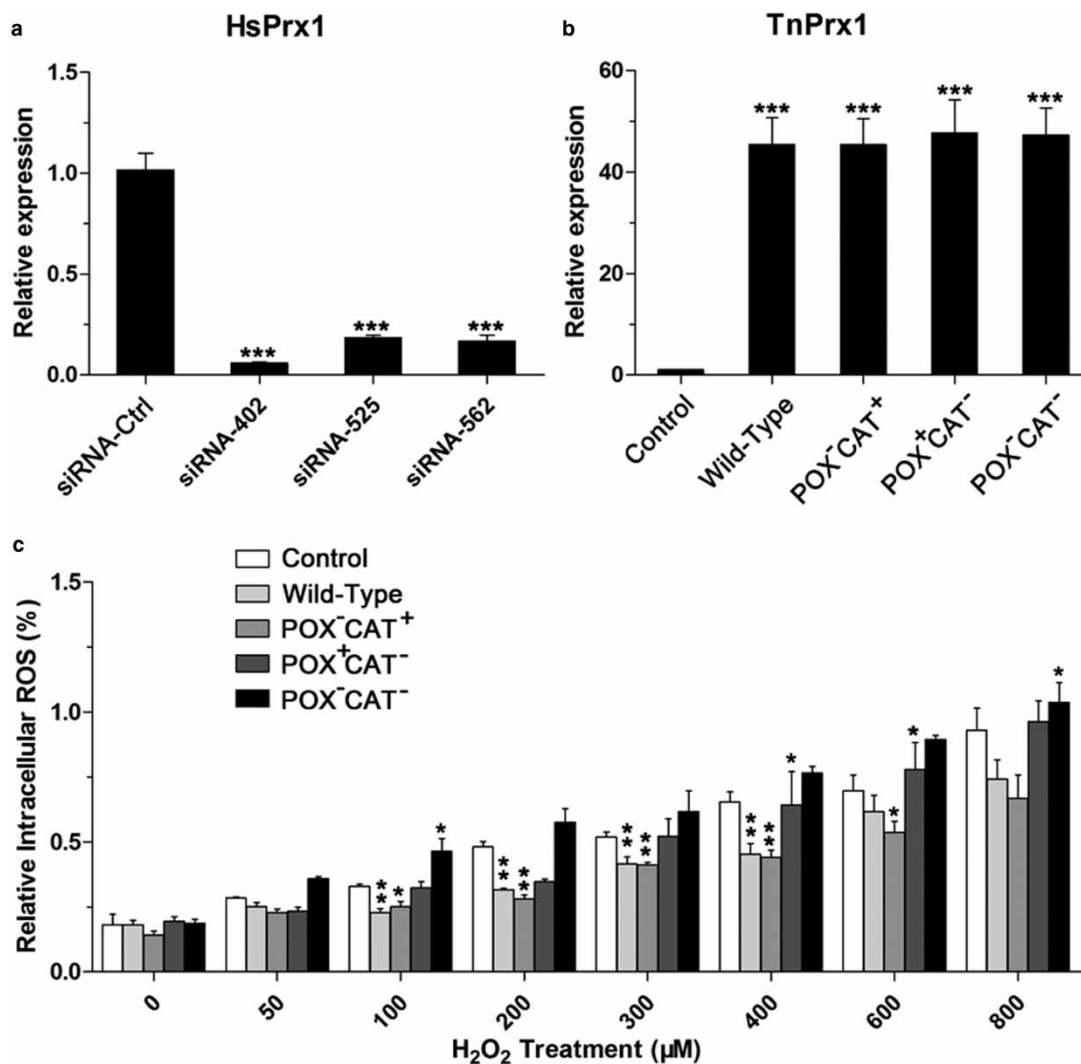
Figure 9. Involvement of TnPrx1 constructs in regulating intracellular ROS (iROS) in wild-type and *HsPrx1*-silienced HEK-293T cells.

(**a**) Interference of *HsPrx1* expression in HEK-293T cells by three siRNA species targeting *HsPrx1*. Negative control used siRNA-Ctrl. The interference efficiency was shown as relative levels of *HsPrx1* transcripts determined by qRT-PCR (real-time quantitative polymerase chain reaction). (**b**) Expression of various TnPrx1 constructs in cells co-transfected with siRNA-402. (**c**) Effects of *TnPrx1* constructs on iROS (intracellular reactive oxygen species) levels in siRNA-402-transfected cells treated with exogenous H_2O_2 as determined by DCFH Dichlorodihydrofluorescein Diacetate fluorescence assay. Cells transfected with siRNA-402 only were used as control. Error bars represent standard deviations (SDs). Asterisks show statistical significances between the experimental and control groups by Student's *t*-test (*$P < 0.05$, **$P < 0.01$ and ***$P < 0.001$). POX = Cys-dependent thioredoxin peroxidase; CAT = Catalase-like activity of peroxiredoxin 1.

in brain cells [47,48]. Moreover, appropriately stimulated polymorphonuclear leukocytes (PMN) and monocytes can produce up to 1.5 nmol of H_2O_2 in 10^4 cells per hour (which is roughly equivalent to >350–450 mM of H_2O_2) if it is not removed and accumulated per hour, given their cell sizes at ~330 and 420 fL [49,50]. In the present study, we have shown that Prx1 acts mainly (if not only) as POX under low-level H_2O_2 environment with high affinity and relatively low capacity (K_m and k_{cat} at ~2.23–4.15 µM and ~0.23 s^{-1}), but as both POX and CAT when H_2O_2 level reaches ~50 µM or higher, where the latter behaves as an allosteric enzyme with activity 10-times higher than the former (K_m and k_{cat} at ~210 µM and 2.3 s^{-1}).
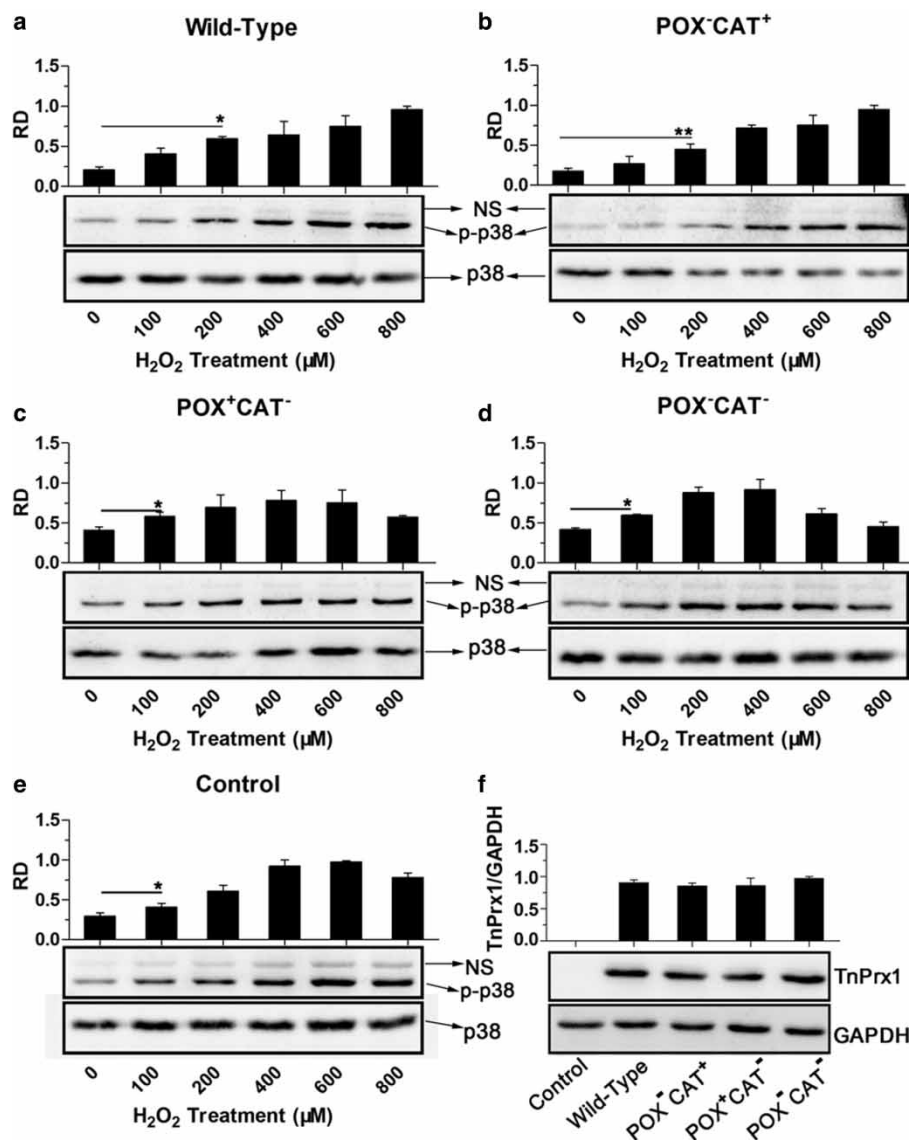
Figure 10. Effects of various *TnPrx1* constructs on the ROS-mediated phosphorylation of p38 MAPK in *HsPrx1*-silienced HEK-293T cells.

(**a–e**) Western blot analysis of total protein extracts from cells co-transfected with *HsPrx1*-siRNA-402 and various *TnPrx1* constructs after the treatment of various concentrations of exogenous H_2O_2 using antibodies specific to p38 and phosphorylated p38 (p-p38) proteins. Control cells were transfected with siRNA-402 only. Representative data from one of the three independent experiments are shown. (**f**) Protein expression of TnPrx1 constructs by Western blot analysis using antibodies specific to His-tag and to human GAPDH (glyceraldehyde-3-phosphate dehydrogenase) (control). An asterisk in each bar chart indicates the lowest concentration of exogenous H_2O_2 yielding statistical significance between H_2O_2-treated cells and untreated controls (*$P < 0.05$, **$P < 0.01$ by Student's *t*-test). RD = relative density.

In vitro transfection experiments also confirmed the functional difference between these two activities, since HEK-293T cells overexpressing WT TnPrx1 and mutant retaining CAT activity were capable of scavenging more iROS than those overexpressing mutants lacking CAT or both POX and CAT activities at low to middle micromolar H_2O_2 levels (Figures 7c and 9c). The levels of exogenous H_2O_2 necessary to produce significant effects on cellular activities, such as on the phosphorylation of p38 in cells transfected with various TnPrx1 mutants, were ∼375–1050 μM or higher (Figure 8), which corresponded to ∼50–150 μM intracellular H_2O_2 based on the model that predicted that intracellular H_2O_2 concentrations were ∼seven-fold or even 10–

PORTLAND PRESS

Table 3. Percentage amino acid identity and similarity of vertebrate Prx1*

	Rat	Mouse	Bovine	Platypus	Chicken	Zebrafinch	Lizard	Frog	Zebrafish	Catfish	Tetraodon	Fugu	Rainbow trout
Human	97/98	95/98	96/98	92/98	88/94	87/94	86/94	84/94	81/92	84/93	79/89	80/90	82/92
Rat		96/100	96/97	91/97	88/93	87/93	86/93	85/92	81/91	84/92	79/88	79/89	82/91
Mouse			95/97	90/97	87/93	87/93	85/94	82/93	79/92	82/92	77/88	77/89	79/91
Bovine				90/97	87/93	88/93	85/93	84/93	80/91	83/92	79/89	79/90	82/92
Platypus					87/95	87/95	89/95	83/94	80/92	82/94	80/90	80/91	81/93
Chicken						97/99	90/97	83/93	83/92	89/96	85/92	85/93	85/93
Zebrafinch							89/97	83/92	82/93	88/96	84/92	84/93	84/93
Lizard								82/92	81/93	82/95	83/91	83/92	80/92
Frog									77/91	80/93	77/90	77/90	77/90
Zebrafish										90/95	83/91	84/92	87/92
Catfish											87/93	88/94	89/94
Tetraodon												98/99	88/94
Fugu													88/95

*Data shown as identity/similarity (%).

100-folds lower than that applied exogenously [48,51,52]. The corresponding intracellular levels of H_2O_2 fell within the levels for physiologically relevant signaling (i.e. 15–150 μM) [52].

Collectively, the existence of a two-fold difference in K_m between Prx1-POX and Prx1-CAT activities enables Prx1 to function on a wider range of ROS concentrations than many other proteins in the cytosol, in which Prx1-POX acts on sub- to lower micromolar iROS normally present in cells, whereas Prx1-CAT (probably along with GPx) and classic CAT enzymes acts on moderate to higher micromolar iROS concentrations that are present in certain types of cells (e.g. some brain and immune cells and/or required for H_2O_2 signaling) (Table 1). The increased oxidative stress in cells with moderate to higher micromolar iROS levels might cause Prx1 to undergo a functional switch from Prx1-POX to Prx1-CAT by hyperoxidation and/or phosphorylation [13–17]. The exact functional connection between Prx1-POX and Prx1-CAT activities and the molecular mechanism underlying the conversion of the two K_m values remains to be clarified. The development of a more sensitive and accurate method for local iROS detection is crucial to this clarification.

However, it is noticeable that although TnPrx1 and HsPrx display CAT-like activity, their catalytic efficiencies are ∼100-fold smaller than those of regular CATs (i.e. $k_{cat}/K_m^{Prx1-CAT}$ at ∼10^4 M^{-1} s^{-1} vs. k_{cat}/K_m^{CAT} at ∼10^6 M^{-1} s^{-1}), which raises the question of whether Prx1-CAT function is critical to organisms, since a higher level of iROS may be quickly scavenged by regular CAT. Prx1 is a cytosol protein, whereas native CATs are typically present in peroxisomes. Data-mining the Multi-Omics Profiling Expression Database (MOPED) (https://www.proteinspire.org/) also reveals that human Prx1 is much more abundant than CAT in most cells/tissues (Supplementary Figure S2a). Therefore, we speculate that the CAT-like activity in Prx1 and possibly in other Prxs may act as one of the first line of scavengers for cytosolic ROS. Prx-CAT may also play more critical role in scavenging and/or regulating ROS in certain cells and tissues that are deficient, or contain extremely low levels of CAT. For example, in human bone, oral epithelium and retina, the CAT protein levels are 132-, 45- and 36-fold less than Prx1 (i.e. 13 vs. 1730, 55 vs. 2490, and 110 vs. 4020 ppm, respectively). Some cancer cells might also take advantage of the Prx1-CAT activity, since the expressions of CAT were deficient or highly down-regulated in many cancer cells [53], whereas those of Prx1 were up-regulated in cancer cells including breast, lung and urinary cancers and hepatocellular carcinoma [54]. The down- and up-regulation of CAT and Prx1 was also clearly supported by comparing the MOPED protein expression profiles between cancer and non-cancer cells (Supplementary Figure S2b). Additionally, we also confirmed by qRT-PCR that the mRNA level of CAT in HEK-293T cells was ∼50–200-fold less than that of Prx1 (Figure 7a).

The Prx-CAT function might also explain how some invertebrates lacking CAT and GPx regulate high levels of intracellular ROS. For example, some parasitic helminths (e.g. *Fasciola hepatica* and *Schistosoma mansoni*)

and roundworms (e.g. filarial parasites), as well as some protozoa (e.g. *Plasmodium* sp.) are deficient in CAT and GPx, but possess highly expressed Prx genes [32,46].

In summary, we observed a CAT-like activity in the pufferfish and human Prx1 proteins that were independent of Cys residue and reductants, but dependent on non-heme mononuclear iron. TnPrx1-CAT activity was capable of regulating intracellular ROS and the ROS-dependent phosphorylation of p38 in transfected HEK-293T cells. These newly discovered features extended our knowledge of Prx1 and provided a new opportunity to further dissect its biological roles.

Abbreviations

3-AT, 3-amino-1,2,4-triazole; CAT, Catalase; DCFH-DA, 2′7′-dichlorodihydrofluorescein diacetate; DMEM, Dulbecco's modified Eagle's medium; DP, 2,2′-dipyridyl; DTT, Dithiothreitol; ECL, Enhanced chemiluminescence; GPx, Glutathione peroxidase; Grx, Glutaredoxin; HBP23, Heme-binding protein 23 kDa; HsPrx, *Homo sapiens* (human) peroxiredoxin; ICP-OES, Inductively coupled plasma optical emission spectroscopy; iROS, Intracellular reactive oxygen species; MAPK, mitogen-activated protein kinase; MOPED, Multi-Omics Profiling Expression Database; ORF, Open reading frame; p38, p38 mitogen-activated protein kinase (MAPK); PMN, Polymorphonuclear leukocytes; POX, Thioredoxin peroxidase; p-p38, Phosphorylated p38 MAPK; Prx, Peroxiredoxin; Prx1-CAT, Catalase-like activity of peroxiredoxin 1; Prx1-POX, Thioredoxin peroxidase activity of peroxiredoxin 1; qRT-PCR, Quantitative reverse transcription-polymerase chain reaction; ROS, Reactive oxygen species; SD, Standard deviation of the mean; SOD, Superoxide dismutase; Srx, Sulfiredoxin; Tiron, 4,5-dihydroxy-1,3-benzene disulfonic acid; TnPrx, *Tetraodon nigroviridis* (green spotted puffer fish) peroxiredoxin; Trx, Thioredoxin; TrxR, Thioredoxin reductase; WT, Wild-type.

Author contribution

J.Z.S., G.Z., C.C.S., W.R.D. contributed to the experimental design. C.C.S., W.R.D., S.T. and L.J.Y. performed most of the experiments and data analysis. J.Z. constructed a cysteine mutant TnPrx1 (POX⁻CAT⁺) and performed protein expression. L.N. cloned the *Prx1* gene of *Tetraodon nigroviridis* and *Homo sapiens*. C.C.S., W.R.D., S.T., G.Z., J.Z.S. participated in manuscript preparation. L.X.X., G.Z., J.Z.S. reviewed and edited the manuscript. All authors read and approved the final manuscript.

Funding

Competing Interests

The Authors declare that there are no competing interests associated with the manuscript.

References

1   Rhee, S. G. (2016) Overview on peroxiredoxin. *Mol. Cells* **39**, 1–5

2   Netto, L. E. and Antunes, F. (2016) The roles of peroxiredoxin and thioredoxin in hydrogen peroxide sensing and in signal transduction. *Mol. Cells* **39**, 65–71

3   Perkins, A., Nelson, K. J., Parsonage, D., Poole, L. B. and Karplus, P. A. (2015) Peroxiredoxins: guardians against oxidative stress and modulators of peroxide signaling. *Trends Biochem. Sci.* **40**, 435–445

4   Rhee, S. G., Kang, S. W., Jeong, W., Chang, T.-S., Yang, K.-S. and Woo, H. A. (2005) Intracellular messenger function of hydrogen peroxide and its regulation by peroxiredoxins. *Curr. Opin. Cell Biol.* **17**, 183–189

5   Rhee, S. G., Woo, H. A., Kil, I. S. and Bae, S. H. (2012) Peroxiredoxin functions as a peroxidase and a regulator and sensor of local peroxides. *J. Biol. Chem.* **287**, 4403–4410

6   Brown, J. D., Day, A. M., Taylor, S. R., Tomalin, L. E., Morgan, B. A. and Veal, E. A. (2013) A peroxiredoxin promotes H₂O₂ signaling and oxidative stress resistance by oxidizing a thioredoxin family protein. *Cell Rep.* **5**, 1425–1435

7   Chae, H. Z., Kim, H. J., Kang, S. W. and Rhee, S. G. (1999) Characterization of three isoforms of mammalian peroxiredoxin that reduce peroxides in the presence of thioredoxin. *Diabetes Res. Clin. Pract.* **45**, 101–112

8   Seo, M. S., Kang, S. W., Kim, K., Baines, I. C., Lee, T. H. and Rhee, S. G. (2000) Identification of a new type of mammalian peroxiredoxin that forms an intramolecular disulfide as a reaction intermediate. *J. Biol. Chem.* **275**, 20346–20354

PORTLAND
PRESS

9   Wang, X., Phelan, S. A., Petros, C., Taylor, E. F., Ledinski, G., Jürgens, G. et al. (2004) Peroxiredoxin 6 deficiency and atherosclerosis susceptibility in mice: significance of genetic background for assessing atherosclerosis. *Atherosclerosis* **177**, 61–70

10   Wood, Z. A., Schröder, E., Robin Harris, J. and Poole, L. B. (2003) Structure, mechanism and regulation of peroxiredoxins. *Trends Biochem. Sci.* **28**, 32–40

11   Chae, H. Z., Chung, S. J. and Rhee, S. G. (1994) Thioredoxin-dependent peroxide reductase from yeast. *J. Biol. Chem.* **269**, 27670–27678

12   Chae, H. Z., Uhm, T. B. and Rhee, S. G. (1994) Dimerization of thiol-specific antioxidant and the essential role of cysteine 47. *Proc. Natl. Acad. Sci. U. S.A.* **91**, 7022–7026

13   Park, J. W., Mieyal, J. J., Rhee, S. G. and Chock, P. B. (2009) Deglutathionylation of 2-Cys peroxiredoxin is specifically catalyzed by sulfiredoxin. *J. Biol. Chem.* **284**, 23364–23374

14   Chae, H. Z., Oubrahim, H., Park, J. W., Rhee, S. G. and Chock, P. B. (2012) Protein glutathionylation in the regulation of peroxiredoxins: a family of thiol-specific peroxidases that function as antioxidants, molecular chaperones, and signal modulators. *Antioxid. Redox Signal.* **16**, 506–523

15   Jang, H. H., Lee, K. O., Chi, Y. H., Jung, B. G., Park, S. K., Park, J. H. et al. (2004) Two enzymes in one: two yeast peroxiredoxins display oxidative stress-dependent switching from a peroxidase to a molecular chaperone function. *Cell* **117**, 625–635

16   Biteau, B., Labarre, J. and Toledano, M. B. (2003) ATP-dependent reduction of cysteine-sulphinic acid by S. cerevisiae sulphiredoxin. *Nature* **425**, 980–984

17   Chang, T.-S., Jeong, W., Woo, H. A., Lee, S. M., Park, S. and Rhee, S. G. (2004) Characterization of mammalian sulfiredoxin and its reactivation of hyperoxidized peroxiredoxin through reduction of cysteine sulfinic acid in the active site to cysteine. *J. Biol. Chem.* **279**, 50994–51001

18   Neumann, C. A., Cao, J. and Manevich, Y. (2009) Peroxiredoxin 1 and its role in cell signaling. *Cell Cycle* **8**, 4072–4078

19   Dong, W.-R., Sun, C.-C., Zhu, G., Hu, S.-H., Xiang, L.-X. and Shao, J.-Z. (2014) New function for Escherichia coli xanthosine phophorylase (xapA): genetic and biochemical evidences on its participation in NAD$^+$ salvage from nicotinamide. *BMC Microbiol.* **14**, 29

20   Guo, F. and Zhu, G. (2012) Presence and removal of a contaminating NADH oxidation activity in recombinant maltose-binding protein fusion proteins expressed in Escherichia coli. *BioTechniques* **52**, 247–253

21   Parejo, I., Petrakis, C. and Kefalas, P. (2000) A transition metal enhanced luminol chemiluminescence in the presence of a chelator. *J. Pharmacol. Toxicol. Methods* **43**, 183–190

22   Kniemeyer, O. and Heider, J. (2001) Ethylbenzene dehydrogenase, a novel hydrocarbon-oxidizing molybdenum/iron-sulfur/heme enzyme. *J. Biol. Chem.* **276**, 21381–21386

23   Park, J., Lee, S., Lee, S. and Kang, S.W. (2014) 2-cys peroxiredoxins: emerging hubs determining redox dependency of Mammalian signaling networks. *Int. J. Cell Biol.* **2014**, 1–10

24   Aggeli, I.-K.S., Gaitanaki, C. and Beis, I. (2006) Involvement of JNKs and p38-MAPK/MSK1 pathways in H$_2$O$_2$-induced upregulation of heme oxygenase-1 mRNA in H9c2 cells. *Cell. Signal.* **18**, 1801–1812

25   Mittler, R., Vanderauwera, S., Gollery, M. and Van Breusegem, F. (2004) Reactive oxygen gene network of plants. *Trends Plant Sci.* **9**, 490–498

26   Panfili, E., Sandri, G. and Ernster, L. (1991) Distribution of glutathione peroxidases and glutathione reductase in rat brain mitochondria. *FEBS Lett.* **290**, 35–37

27   Bendayan, M. and Reddy, J. K. (1982) Immunocytochemical localization of catalase and heat-labile enoyl-CoA hydratase in the livers of normal and peroxisome proliferator-treated rats. *Lab Invest.* **47**, 364–369

28   Benfeitas, R., Selvaggio, G., Antunes, F., Coelho, P.M. and Salvador, A. (2014) Hydrogen peroxide metabolism and sensing in human erythrocytes: A validated kinetic model and reappraisal of the role of peroxiredoxin II. *Free Radic. Biol. Med.* **74**, 35–49

29   Matte, A., Low, P.S., Turrini, F., Bertoldi, M., Campanella, M.E., Spano, D. et al. (2010) Peroxiredoxin-2 expression is increased in β-thalassemic mouse red cells but is displaced from the membrane as a marker of oxidative stress. *Free Radic. Biol. Med.* **49**, 457–466

30   Lee, T.-H., Kim, S.-U., Yu, S.-L., Kim, S. H., Park, D. S., Moon, H.-B. et al. (2003) Peroxiredoxin II is essential for sustaining life span of erythrocytes in mice. *Blood* **101**, 5033–5038

31   Han, Y.-H., Kwon, T.-H., Kim, S.-U., Ha, H.-L., Lee, T.-H., Kim, J.-M. et al. (2012) Peroxiredoxin I deficiency attenuates phagocytic capacity of macrophage in clearance of the red blood cells damaged by oxidative stress. *BMB Rep.* **45**, 560–564

32   Henkle-Dührsen, K. and Kampkötter, A. (2001) Antioxidant enzyme families in parasitic *nematodes. Mol. Biochem. Parasitol.* **114**, 129–142

33   Knoops, B., Loumaye, E. and Van Der Eecken, V. (2007) Evolution of the peroxiredoxins. *Subcell. Biochem.* **44**, 27–40

34   Choi, H.-J., Kang, S. W., Yang, C.-H., Rhee, S. G. and Ryu, S.-E. (1998) Crystal structure of a novel human peroxidase enzyme at 2.0 Å resolution. *Nat. Struct. Biol.* **5**, 400–406

35   Hall, A., Nelson, K., Poole, L. B. and Karplus, P. A. (2011) Structure-based insights into the catalytic power and conformational dexterity of peroxiredoxins. *Antioxid. Redox Signal.* **15**, 795–815

36   Baek, J. Y., Han, S. H., Sung, S. H., Lee, H. E., Kim, Y.-M., Noh, Y. H. et al. (2012) Sulfiredoxin protein is critical for redox balance and survival of cells exposed to low steady-state levels of H$_2$O$_2$. *J. Biol. Chem.* **287**, 81–89

37   Alfonso-Prieto, M., Vidossich, P. and Rovira, C. (2012) The reaction mechanisms of heme catalases: an atomistic view by ab initio molecular dynamics. *Arch. Biochem. Biophys.* **525**, 121–130

38   Hirotsu, S., Abe, Y., Okada, K., Nagahara, N., Hori, H., Nishino, T. et al. (1999) Crystal structure of a multifunctional 2-Cys peroxiredoxin heme-binding protein 23 kDa/proliferation-associated gene product. *Proc. Natl. Acad. Sci. U.S.A.* **96**, 12333–12338

39   Lechardeur, D., Fernandez, A., Robert, B., Gaudu, P., Trieu-Cuot, P., Lamberet, G. et al. (2010) The 2-Cys peroxiredoxin alkyl hydroperoxide reductase c binds heme and participates in its intracellular availability in Streptococcus agalactiae. *J. Biol. Chem.* **285**, 16032–16041

40   Koehntop, K. D., Emerson, J. P. and Que, Jr, L. (2005) The 2-His-1-carboxylate facial triad: a versatile platform for dioxygen activation by mononuclear non-heme iron(II) enzymes. *J. Biol. Inorg. Chem.* **10**, 87–93

41   Andreini, C., Bertini, I., Cavallaro, G., Najmanovich, R. J. and Thornton, J. M. (2009) Structural analysis of metal sites in proteins: non-heme iron sites as a case study. *J. Mol. Biol.* **388**, 356–380

42   Delwiche, E. A. (1961) Catalase of pediococcus cerevisiae. *J. Bacteriol.* **81**, 416–418

43   Johnston, M. A. and Delwiche, E. A. (1965) Isolation and characterization of the cyanide-resistant and azide-resistant catalase of lactobacillus plantarum. *J. Bacteriol.* **90**, 352–356

44 Whittaker, J. W. (2012) Non-heme manganese catalase – the 'other' catalase. *Arch. Biochem. Biophys.* **525**, 111–120

45 Karplus, P. A. and Hall, A. (2007) Structural survey of the peroxiredoxins. *Subcell. Biochem.* **44**, 41–60

46 Robinson, M. W., Hutchinson, A. T., Dalton, J. P. and Donnelly, S. (2010) Peroxiredoxin: a central player in immune modulation. *Parasite Immunol.* **32**, 305–313

47 Qutub, A. A. and Popel, A. S. (2008) Reactive oxygen species regulate hypoxia-inducible factor 1α differentially in cancer and ischemia. *Mol. Cell. Biol.* **28**, 5106–5119

48 Avshalumov, M. V., Bao, L., Patel, J. C. and Rice, M. E. (2007) H_2O_2 signaling in the nigrostriatal dopamine pathway via ATP-sensitive potassium channels: issues and answers. *Antioxid. Redox Signal.* **9**, 219–231

49 Szatrowski, T. P. and Nathan, C. F. (1991) Production of large amounts of hydrogen peroxide by human tumor cells. *Cancer Res.* **51**, 794–798

50 Nibbering, P. H., Zomerdijk, T. P., Corsèl-Van Tilburg, A. J. and Van Furth, R. (1990) Mean cell volume of human blood leucocytes and resident and activated murine macrophages. *J. Immunol. Methods.* **129**, 143–145

51 Antunes, F. and Cadenas, E. (2000) Estimation of H_2O_2 gradients across biomembranes. *FEBS Lett.* **475**, 121–126

52 Rice, M. E. (2011) H_2O_2: a dynamic neuromodulator. *Neuroscientist* **17**, 389–406

53 Wang, D., Li, F., Chi, Y. and Xiang, J. (2012) Potential relationship among three antioxidant enzymes in eliminating hydrogen peroxide in penaeid shrimp. *Cell Stress Chaperones* **17**, 423–433

54 Cai, C.-Y., Zhai, L.-L., Wu, Y. and Tang, Z.-G. (2015) Expression and clinical value of peroxiredoxin-1 in patients with pancreatic cancer. *Eur. J. Surg. Oncol.* **41**, 228–235

55 Matsumoto, M., Sudo, T., Saito, T., Osada, H. and Tsujimoto, M. (2000) Involvement of p38 mitogen-activated protein kinase signaling pathway in osteoclastogenesis mediated by receptor activator of NF-κB ligand (RANKL). *J. Biol. Chem.* **275**, 31155–31161

56 Reyes-Moreno, C., Girouard, J., Lapointe, R., Darveau, A. and Mourad, W. (2004) CD40/CD40 homodimers are required for CD40-induced phosphatidylinositol 3-kinase-dependent expression of B7.2 by human B lymphocytes. *J. Biol. Chem.* **279**, 7799–7806

57 Madrid, L. V., Mayo, M. W., Reuther, J. Y. and Baldwin, Jr, A. S. (2001) Akt stimulates the transactivation potential of the relA/p65 subunit of NF-κB through utilization of the IκB kinase and activation of the mitogen-activated protein kinase p38. *J. Biol. Chem.* **276**, 18934–18940